Systems of atoms with a short-range interaction

B. M. Smirnov

Institute of High Temperatures, Russian Academy of Sciences, Moscow
(Submitted 25 March 1992)
Usp. Fiz. Nauk **162**, 97–150 (December 1992)

The properties of systems consisting of classical atoms with a short-range interaction and the processes occurring in them are studied. An asymptotic theory is presented for the transport coefficients and other parameters of a gas, which exploits the steepness of the interaction potential of the atoms in the repulsive region. A comparison of the parameters of various condensed inert gases shows that these parameters can be expressed in terms of the interaction potential between two atoms. On the basis of a model of close-packing of the atoms analyses are made of the properties of large clusters, the surface energy of condensed and porous systems, the surface tension of liquids and liquid metals, and of the solid-liquid phase transition.

1. INTRODUCTION

An interaction between atoms and molecules is regarded as short-range when it comes into play only when the distance between the particles is small. In a bound system of many atoms and molecules the short-range interaction occurs between atoms that are nearest neighbors. Ordinarily, it is the short-range interaction that acts between the atoms and molecules of a gas. For example, inert gas atoms have a closed electron shell, so that the exchange interaction between two atoms due to the overlap of the electron shells causes a strong repulsion. The attraction at large internuclear distances is due to weak dispersion forces. Therefore, the interaction potential between two atoms is characterized by a strong repulsion when the atoms are close together and a shallow well at distances comparable to atomic dimensions. In denoting this interaction as short range, we assume that in the region of attraction the interaction potential is characterized by a narrow well and the absence of any long-range interaction.

This form of the interaction potential is reflected in various properties of atomic systems. Such a system of atoms is well described by models in which atoms are replaced by balls. Then the properties of a gas that are determined by atomic collisions (such as the transport coefficients) can be analyzed with the use of a hard-ball or hard-sphere model for the colliding atoms.[1-3] In the analysis of the properties of bound systems of atoms (polyatomic molecules, clusters, the condensed state), it is convenient to model the atoms as balls, considering only the interaction between nearest neighbors. In this case, the short-range interaction corresponds to pairwise interactions between atoms in the condensed system.

There is still another property of a condensed system of atoms with this type of interaction. Because of the absence of long-range interactions no stresses arise in such a system. Moreover, because of the shallowness of the well in the interaction potential, the interaction between two neighboring atoms does not depend on whether these atoms interact with other atoms. This means that vacancies in the system have no effect on the interaction of the atoms adjacent to them, and consequently the vacancies do not interact among themselves until they have a common boundary. All these factors underscore the simplicity and convenience of this model.

Therefore, in the analysis of the properties of a system of atoms with a short-range interaction, these atoms can conveniently be described by ball models. The accumulated experience in this regard can be summarized as follows. First, the short-range interaction of atoms applies to real systems, the interaction of inert gas atoms and gas molecules. For these cases the ball models can be modified by means of a small parameter that takes into account either the steepness of the repulsive potential or the smallness of the depth and width of the well in the interaction potential of the two atoms. In this way this model is able to describe real systems of atoms. Second, the results of the ball models are relatively simple, and therefore they can be used to estimate the properties of more complicated systems.

This review presents an analysis of the properties of systems that are composed of atoms with a short range interaction, and a number of models that describe these systems are considered. These models are used to analyze the properties of various atomic systems.

2. GAS SYSTEMS

2.1. Interaction potential of the atoms

In the analysis of gas systems consisting of atoms with a short-range interaction, the item of foremost interest is the collision of two atoms. In examining these collision processes we assume that in the collision the atoms behave as classical particles. This assumption is valid, for example, in

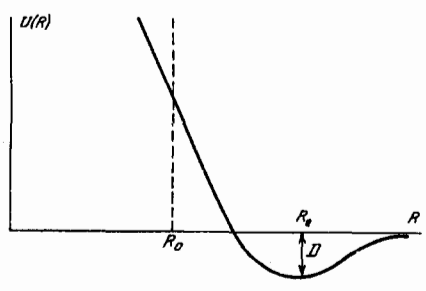

FIG. 1. Interaction potential between two atoms. The dashed line is the model potential corresponding to the hard-sphere model.

 0038-5670/92/121052-28$03.00

TABLE I. Internuclear distance R_e (Å) corresponding to the minimum of the interaction potentials.[4-12]

Interacting atoms	He	Ne	Ar	Kr	Xe
He	2.97	3,2	3,5	3,8	4,1
Ne	—	3,09	3,5	3,7	3,8
Ar	—	—	3,76	3,9	4,1
Kr	—	—	—	4,01	4,3
Xe	—	—	—	—	4,36

the calculation of the transport coefficients in any inert gas or molecular gas under normal conditions (i.e., a pressure of 1 atm and a temperature $T = 273$ K).

The parameters of the gas system are determined by the interaction potential of its atoms. Figure 1 shows the shape of the interaction potential between two atoms. The features of the potential for the short-range interaction between the atoms are associated with the shallowness of the potential well and the steep variation of the potential as a function of the internuclear distance in the repulsive part of the potential. Since we shall henceforth be concerned mainly with inert gases as a real case corresponding to the short-range interaction of the atoms, Tables I–III list the parameters of molecules consisting of two atoms of an inert gas.[4-14] It can be seen that the depth of the well is small compared to characteristic atomic energies ($me^4/\hbar^2 = 27.2$ eV) and to the characteristic dissociation energies of stable molecules, while the equilibrium distance is large compared to characteristic atomic dimensions ($\hbar^2/me^2 = 0.53 \cdot 10^{-8}$ cm). The accuracy in the listed parameters is better than 10% for the binding energies and better than 3% for the equilibrium internuclear distances.

Table III lists the logarithmic derivative in the repulsive region of the potential

$$n = \frac{d\ln U(R)}{d\ln R}, \tag{1}$$

where $U(R)$ is the interaction potential at a distance R between the nuclei. This quantity is given for an energy where the interaction potential is 0.3 eV, which is considerably more than the depth of the well in the interaction potential of the atoms considered. The values listed were obtained from the data of Leonas.[14] As is shown, $n \gg 1$. This result can be obtained from general considerations. The basic function in the potential of the exchange interaction is an exponential dependence for two identical atoms at large internuclear distances proportional to $\psi^4(R/2)$ (Refs. 15–17), where $\psi(r)$ is the wave function of a valence electron at a distance r from the nucleus. Thus,

$$U(R) \exp(-\gamma R), \tag{2}$$

where the parameter γ in atomic units is equal to $(2I)^{1/2}$ and I is the ionization potential of the atom. Since $\gamma \sim 1$ and the characteristic internuclear distance in atomic units is somewhat greater than unity, the logarithmic derivative is relatively large. This result comes from the fact that in the region of interest the exchange interaction potential is much smaller than characteristic atomic energies. Therefore, the argument of the exponential is relatively large. Table IV lists the values of the parameter $2\gamma R_e$, where R_e is the equilibrium internuclear spacing in a molecule consisting of identical atoms with a repulsive interaction potential of 0.3 eV.

2.2. Cross section for collisions of atoms

The transport processes in gases are controlled by collisions of the atoms, with the collision cross section being related to the repulsive part of the interaction potential. Since the potential varies rapidly with distance in this region, it can be replaced by an infinitely high wall in the zero-order approximation (Fig. 1). The corresponding model of scattering of the atoms is called the hard-sphere model.[1-3] In this model the relative motion of the atoms is free at internuclear distances $R > R_0$, where R_0 is the radius of the hard sphere. The spheres are reflected at $R = R_0$ (Fig. 2).

Let us determine the differential scattering cross section of the atoms in the hard-sphere model. Figure 2 shows that the impact parameter ρ of the collision is related to the scattering angle ϑ by the relation $\rho = R_0 \cos(\vartheta/2)$. The cor-

TABLE II. Depth of well, D_0 (meV) in the potential of the interacting atoms.[4-12]

Interacting atoms	He	Ne	Ar	Kr	Xe
He	0.93	1,6	1,8	2,5	2,5
Ne	—	3,7	6,0	6,0	6,1
Ar	—	—	12,2	15	15
Kr	—	—	—	17,2	19
Xe	—	—	—	—	24

TABLE III. Values of the parameter n in formula (1) of a repulsive potential equal to 0.3 eV (data of Leonas[14]). The parentheses indicate the internuclear distances for the potential in units of 0.1 nm.

Interacting atoms	He	Ne	Ar	Kr	Xe
He	5.86 (1,58)	5,61 (1,87)	5,15 (2,31)	5,52 (2,48)	5,2 (2,50)
Ne	—	7,65 (2,07)	6,58 (2,42)	7,65 (2,59)	6,76 (2,64)
Ar	—	—	6,06 (2,85)	6,92 (3,16)	5,9 (3,44)
Kr	—	—	—	7,7 (2,99)	7,1 (3,08)
Xe	—	—	—	—	6,35 (3,18)

responding differential scattering cross section is

$$d\sigma = 2\pi\rho d\rho = \frac{\pi R_0^2}{2} d\cos\vartheta. \quad (3)$$

As can be seen, the differential scattering cross section depends on the scattering angle. Using formula (3) one can find the integrated large-angle scattering cross section, in terms of which the kinetic transport coefficients are expressed. The transport, or diffusion scattering cross section is

$$\sigma^{(1)} = \int(1 - \cos\vartheta)\, d\sigma = \pi R_0^2. \quad (4)$$

The scattering cross section that figures in the expression for the heat conductivity and viscosity of a gas is

$$\sigma^{(2)} = \int(1 - \cos^2\vartheta)\, d\sigma = 2\pi R_0^2/3. \quad (5)$$

Within the hard-sphere model the integrated collision cross sections do not depend on the velocities of the colliding particles. Therefore, the properties of the hard-sphere model are related to the fact that the differential cross section for the scattering of particles in this model does not depend on the scattering angle or on the velocities of the particles, while the integrated scattering cross sections do not depend on the velocities of the particles.

From the scattering cross section it is possible to determine the kinetic transport coefficients in gases. Let us represent the most commonly used transport coefficients, the diffusion coefficient D, the thermal conductivity $\varkappa$, and the viscosity η in the Chapman–Enskog approximation. The error incurred in this approximation is considerably less than the errors due to the indeterminacy in the interaction potential of real atoms. For this reason, the error in the Chapman–Enskog approximation will not be discussed. We have[2,3]

$$D = 3(\pi T)^{1/2}/8N\sigma_1(2\mu)^{1/2}, \quad (6)$$

$$\varkappa = 25(\pi T)^{1/2}/32M^{1/2}\sigma_2, \quad (7)$$

$$\eta = 5(\pi TM)^{1/2}/24\sigma_2. \quad (8)$$

Here T is the gas temperature, N is the atomic density of the gas, M is the mass of a gas atom, μ is the reduced mass of the diffusing atoms and the gas atom (in the case of self-diffusion, $\mu = M/2$). Here and below, the temperature will be expressed in energy unity, and so the Boltzmann constant will be omitted. For the averaged cross sections σ_1 and σ_2 the following formula is used for averaging over the Maxwellian distribution of the velocities of the atom ($i = 1,2$):

$$\sigma_i = \frac{1}{2}\int x^2 e^{-x}\sigma^{(i)}(x)dx, \quad (9)$$

where $x = \mu v^2/2T$ is the dimensionless energy, and for the integrated cross sections $\sigma^{(1)}$ and $\sigma^{(2)}$ the following method is used for integrating over the angle in accordance with formulas (4) and (5):

$$\sigma^{(1)} = \int(1 - \cos\vartheta)\, d\sigma, \quad (10)$$

$$\sigma^{(2)} = \int(1 - \cos^2\vartheta)\, d\sigma. \quad (11)$$

For the hard-sphere model the integrated scattering cross sections are given by formulas (4) and (5); $\sigma^{(1)} = \pi R_0^2$, and $\sigma^{(2)} = 2\pi R_0^2/3$. Because these cross sec-

TABLE IV. Values of the exponent in the exchange interaction potential corresponding to a repulsive potential of 0.3 eV for two identical atoms.

	He	Ne	Ar	Kr	Xe
$2\gamma R_e$	18.0	9,8	11,5	11,5	11,3

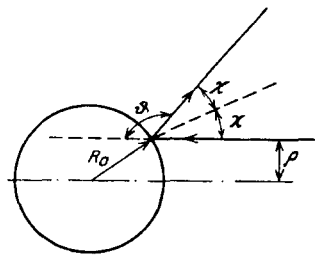

FIG. 2. Scattering of atoms in the hard-sphere model. The heavy lines with arrows are the trajectories of the atoms in the center of mass system. R_0 is the radius of the hard sphere, ρ is the impact parameter, and ϑ is the scattering angle.

tions do not depend on the velocity of collision, the averaged cross sections that enter into the expression for the kinetic coefficients are

$$\sigma_1 = \pi R_0^2, \sigma_2 = 2\pi R_0^2/3. \quad (12)$$

In this way, by substituting the interaction potential between the atoms by an infinite-wall potential (Fig. 1), we can determine the transport coefficients in a gas.

2.3. Modified hard-sphere model

The use of the hard-sphere model brings up the question of how to choose the radius of the sphere. If we start from the real interaction potential, it is obvious that this radius is given by the relation

$$U(R_0) = a\varepsilon, \quad (13)$$

where ε is the collision energy in the center of mass system and the numerical parameter is $a \sim 1$. We note that for a steeply varying repulsive interaction potential the chosen interaction radius R_0 depends only weakly on the parameter a. If this parameter is changed by a factor of k, the relative change in the interaction radius is $\ln k/n$, where n is given by formula (1). It thus follows that when the interaction potential varies steeply, so that $n \gg 1$, this change in the interaction radius is relatively small.

With these results in mind we can set up a perturbation theory, using as the zero-order approximation the hard-sphere model with an interaction radius given by formula (13), with $a = 1$ and with $1/n$ as the small parameter. If we retain only two terms in the perturbation theory so constructed, we obtain the so-called modified hard-sphere model.[16] The modified model retains the simplicity of the hard-sphere model. Its formulas have the same form, but the coefficient a in formula (13) is quite distinct for each integrated cross section.

It is clear that in the modified hard-sphere model the differential scattering cross section (3) retains the same form but the interaction radius R_0 now becomes $R_0 + (F(\vartheta)/n)$, where the first term does not depend on the scattering angle ϑ. Accordingly, the integrated cross sections in the modified hard-sphere model have the same form as in the hard-sphere model, with the interaction radius of these cross sections being given by formula (13) with the numerical value of the coefficient a specific for each type of cross section.

In the Appendix the scattering angle and the integrated scattering cross sections are calculated for the modified hard-sphere model. Although this derivation has been carried out previously,[16,18] it is convenient to reproduce it here in order to present a complete picture. The expressions for the integrated cross sections in the modified hard-sphere model are[19-21]

$$\sigma^{(1)} = \int (1 - \cos\vartheta)\, d\sigma = \pi R_1^2, \; U(R_1) = 0.89\varepsilon, \quad (14)$$

$$\sigma^{(2)} = \int (1 - \cos^2\vartheta)\, d\sigma = 2\pi R_2^2/3, \; U(R_2) = 0.23\varepsilon, \quad (15)$$

$$\sigma_1 = \pi r_1^2, \; U(r_1) = 2.25T, \quad (16)$$

$$\sigma_2 = 2\pi r_2^2/3, \; U(r_2) = 0.83T; \quad (17)$$

where ε is the energy of the colliding atoms in the center of mass system, T is the gas temperature, and the cross sections $\sigma_1(T)$ and $\sigma_2(T)$ are used in expressions (6)–(8) for the kinetic coefficients. The assumption that the average cross sections Eq. (9) are determined by the repulsive part of the interaction potential is equivalent to the fulfillment of the criterion

$$D \ll 2T,$$

where D is the depth of the well in the attractive potential of the atoms.

Within the modified hard-sphere model the exact form of the repulsive potential is unimportant. The use of the logarithmic derivative of the interaction potential means that we are in fact assuming that the interaction potential is an exponential function of the distance between atoms and that the range of distances in which the interaction potential is comparable with the collision energy of the atoms is relatively narrow. Since this is the interaction range and, consequently, range of distances between the atoms in which the trajectories of the colliding atoms are altered, the specific form of the interaction potential far from this region is unimportant.

Let us consider the contribution to the cross section from the discarded terms, that is, the question of the accuracy of the modified hard-sphere model. To do so we compare the results of an exact calculation of the scattering cross section for the potential $U(R) = CR^{-n}$ (Refs. 3, 22–25) with formulas (13)–(16), which come from the modified hard-sphere model. For this potential the dependence of the cross section on the energy of the atoms (or the gas temperature for the average cross sections) is of the form $\sigma \sim \varepsilon^{-2/n}$ where this dependence also corresponds to the modified hard-sphere model. Therefore, the ratio of the cross sections (the accurate one and the approximate one) does not depend on the collision energy. The ratios of the cross sections are given in Table V, where the subscript *as* (asymptotic) is used for the modified hard-sphere model and the subscript *ex* is used for the exact calculations. As can be seen, for collisions of inert gas atoms in the range of energies corresponding to the data of Table III, the modified hard-sphere model is accurate to about 5%. The cross sections that are averaged over the Maxwellian energy distribution of the atoms have the same accuracy.

Hence, the short-range interaction of the atoms provides a small parameter associated with the steep variation in the interaction potential in the repulsive part of the potential. It is therefore possible to obtain simple expressions for the scattering cross section, taking the hard-sphere model as a basis and constructing a perturbation theory with a small

TABLE V. Ratio of the elastic scattering cross sections for the interaction potential $U(R) = CR^{-n}$ between two atoms, calculated by the modified hard-sphere model (formulas (14)–(17)) to the exact values.[3,22–25]

	$n=4$	6	8	10	12	14
$\sigma_{as}^{(1)}/\sigma_{ex}^{(1)}$	0,888	0,936	0,953	0,969	0,972	0,974
$\sigma_{as}^{(2)}/\sigma_{ex}^{(2)}$	1,127	1,056	1,025	1,016	1,010	1,008

parameter that is the inverse of the steepness of the interaction potential between the atoms.

For a demonstration of the possibilities of the modified hard sphere model Figs. 3–7 show the results of calculations of transport coefficients using this method. The calculations themselves are very simple. In particular, the heat conductivity $\varkappa$ as a function of the temperature T in accordance with formulas (7) and (17) is

$$\varkappa(T) = CT^{(1/2)+(2/n)},$$

where n is the logarithmic derivative of the repulsive interaction potential (1). The accuracy of the result is in general determined by the accuracy of the specification of the potential, which is estimated to be about 30%. In these calculations the interaction potentials of the individual atoms were obtained from the measurements of Leonas and his coworkers[26,27] and for the He–Ar interaction potential the data of Danielson and Keil[28] were used. In addition, a comparison was made in the region of high temperatures corresponding to the measured region of the interaction potential, and where the attractive region of the interaction potential plays no role whatever. The comparison was made with the recommended values of Vargaftik and his coworkers,[29,30] obtained with allowance for existing experiments and calculations. The calculations within the modified hard-sphere model are estimated to be accurate to 10%.

To summarize, the modified hard-sphere model employs an expansion of the collision parameters in a small parameter that is related to the steep variation of the repulsive potential as a function of the distance between the colliding atoms. This model gives a good description of the various kinetic coefficients for gases for which the exchange interaction between the atoms is repulsive.

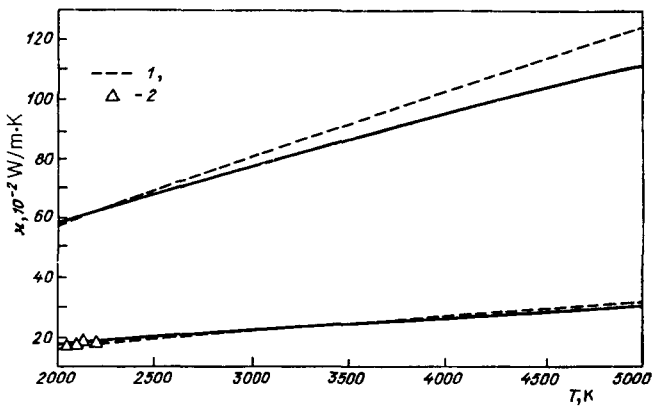

FIG. 3. Thermal conductivity of helium and neon. The solid curves show the values given in Ref. 29; *1*) calculated from formulas (7) and (17); *2*) experiment of Ref. 34.

2.4. Parameters of a gas with a short-range interaction between atoms

The steep variation of the repulsive interaction potential between the atoms makes it possible to analyze not only the collisions of atoms, but also the cases where the result is determined by the interaction itself. Let us consider an example of this sort—the equation of state in a gas with a high temperature and low density, which, when the first term is retained in the expansion in the low density, has the form (see, e.g., Ref. 35)

$$p = NT(1 + NB); \tag{18}$$

where p is the gas pressure, T is the gas temperature, N is the density of the atoms in the gas, and B is the second virial coefficient

$$B(T) = (1/2)\int \left[1 - \exp(-U(R)/T)\right] dR, \tag{19}$$

where $U(R)$ is the interaction potential between two atoms, and R is the distance between them. In this case, the thermal energy of the atoms exceeds the depth of the well in their interaction potential. Therefore, the virial coefficient is determined by the repulsive part of the interaction, and according to formula (19) is

$$B(T) = 2\pi R_0^3/3, \quad U(R_0) = cT \tag{20}$$

and the value of the dimensionless coefficient c is ~ 1. To determine the value of the coefficient c we calculate the integral in Eq. (19) for the interaction potential $U(R) = AR^{-n}$ and go to the limit $n \to \infty$. We have

$$B = \frac{2\pi}{3}\left(\frac{A}{T}\right)^{3/n}\Gamma\left(1 + \frac{3}{n}\right),$$

so that the coefficient in formula (20) is

$$c = \lim_{n\to\infty}\left[\Gamma(1 + (3/n))\right]^{-n/3} = \exp(-\psi(1)) = e^C = 1.78, \tag{21}$$

where $\psi(1)$ is the logarithmic derivative of the gamma function, and $C = 0.577$ is Euler's constant. So we find that here too, we arrive at the same form of result for the equation of state of a gas, Eq. (20), as is given by the modified hard-sphere model for the scattering of atoms.

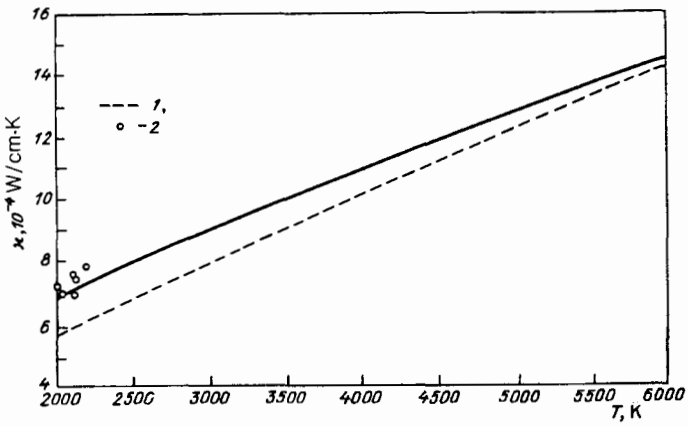

FIG. 4. Thermal conductivity of argon. The solid curve shows the values given in Ref. 29; *1*) calculated from formulas (7) and (17); *2*) experiment of Ref. 34.

Up to this point we have considered the interaction of atoms in a rarefied gas. There the effects are governed by the pairwise interaction and the repulsive part of the potential. In a dense gas the region of attraction of the atoms plays a principal role. An important fact is that in such a system of atoms with a short range interaction one can always limit the analysis to pairwise interactions between the atoms, so that the parameters of the gas can be expressed in terms of the parameters of the pair potential of the interaction in the region of attraction between the atoms. To demonstrate this fact, Table VI shows the values of the critical temperature, pressure, and density of the inert gases.[36-38] If it is assumed that these parameters are determined in the region of attraction in the pair-wise interaction between the atoms, then the critical parameters of the inert gas are expressed in terms of the parameters of a diatomic molecule—the dissociation energy D, the equilibrium distance R_e, and the atomic mass m. From these parameters we can construct only one combination of a given dimensionality, in particular, the pressure $p_0 = D/R_e^3$ and the density $\rho_0 = m/R_e^3$. The data in Table VI show that to a good precision these values are proportional to the measured critical parameters of the inert gas. A statistical analysis of the critical parameters of the inert gases gives $p_{cr} = (0.131 \pm 0.001)p_0$, $T_{cr} = (1.04 \pm 0.02)D$, and $\rho_{cr} = (0.301 \pm 0.001)\rho_0$.

Yet another example of this kind refers to the saturated vapor pressure, which is determined by the parameters of the interaction of the atoms at the surface of a condensed system. Figure 8 shows the temperature dependence of the saturated vapor pressure of inert gases in dimensionless variables. From this figure we can appreciate the degree to which the scaling laws are satisfied in this case.

3. CONDENSED SYSTEMS OF ATOMS

3.1. The parameters and the structure of crystals

While the main properties and the behavior of a gas consisting of atoms with a short-range interaction between them are determined by the repulsive part of the interaction potential, the behavior of a bound state of a system of these atoms, on the contrary, is controlled by the more distant, attractive part of the interaction potential. In the condensed state the atoms with a short range interaction form structures that correspond to close packing of the atoms. In these structures the atoms can be considered as balls with a radius R_e, where R_e is the equilibrium distance between the atoms in a dimer (a diatomic molecule). Since the parameters of

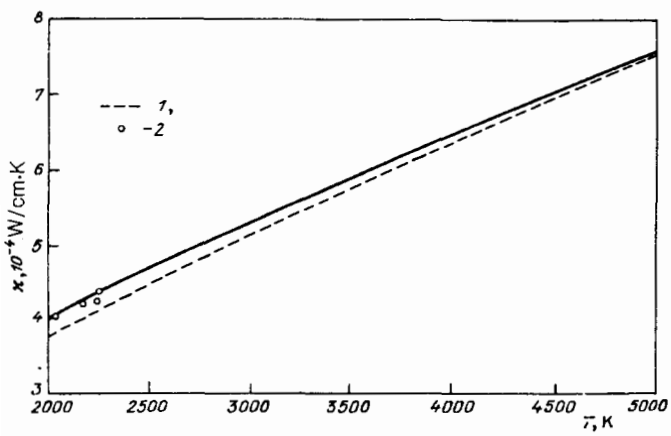

FIG. 5. Thermal conductivity of krypton. The solid curve shows the values given in Ref. 29; *1*) calculated from formulas (7) and (17); *2*) experiment of Ref. 34.

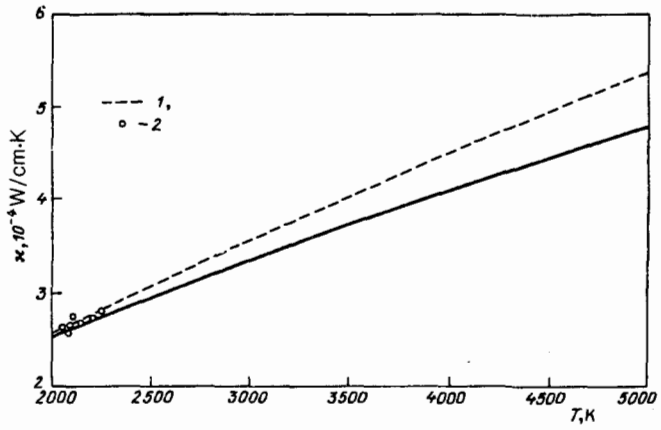

FIG. 6. Thermal conductivity of xenon. The solid curve shows the values given in Ref. 29; *1*) calculated from formulas (7) and (17); *2*) experiment of Ref. 34.

the condensed system of atoms are determined by their pair-wise interaction, these parameters can be expressed in terms of the parameters of the pair-wise interaction in the diatomic molecule, the dissociation energy D of the dimer, and the equilibrium internuclear distance R_e.

In the subsequent analysis of a condensed system of atoms we shall neglect quantum-mechanical effects and assume that the temperature of the system is relatively low. It is possible to neglect quantum-mechanical effects if $\Delta H \gg \hbar\omega_D$, where $\hbar\omega_D$ is the Debye energy corresponding to the condensed system and ΔH is the energy of sublimation, i.e., the energy per atom required for the transformation of the condensed system into a gas of atoms. This condition is violated in the case of helium and is fairly well satisfied for neon. Nonetheless, we shall neglect quantum corrections and assume that the systems are classical. The parameters of the condensed state of the inert gases are listed in Table VII.

These properties of a condensed system of atoms do not include the dependence of the parameters on the pressure, and so the parameters that are analyzed in this paper refer to atmospheric pressure of the inert gases.

Two consequences emerge from the model assumptions that we use, according to which the condensed structures are held together as a result of the interaction between nearest neighbors. First, these atoms form close-packed structures. Second, the nature of the interaction between atoms in the condensed state is the same as that in the dimer. The validity of the latter statement can be demonstrated by a comparison of the interatomic distance (R_e) in a dimer with the distance a between nearest neighbors in an inert gas crystal (Tables I and VII). As can be seen, these values agree within 2%. Since each atom in a crystal with close packing has 12 nearest neighbors, the sublimation energy per atom of the crystal in the case of a short-range interaction between atoms is

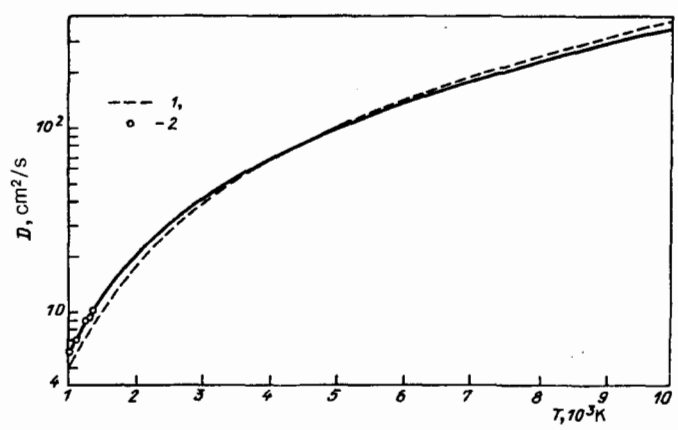

FIG. 7. Diffusion coefficient of helium in argon. The solid curve shows the values given in Ref. 30; *1*) calculated from formulas (6) and (16); *2*) experiment of Refs. 31–33.

TABLE VI. Critical parameters of inert gases[36–38].

	Ne	Ar	Kr	Xe
Critical temperature T_{cr}, K	44,4	150,7	20,4	289,8
Critical pressure p_{cr}, MPa	2,653	4,860	5,510	5,842
Critical density ρ_{cr}, g/cm^3	0,484	0,535	0,919	1,11
$p_0 = D/R_e^3$, MPa	20,1	36,7	42,7	44,4
$\rho_0 = m/R_e^3$, g/cm^3	1,606	1,764	3,051	3,718
T_{cr}/D	1,03	1,06	1,05	1,04
ρ_{cr}/p_0	0,132	0,132	0,129	0,132
ρ_{cr}/ρ_0	0,301	0,303	0,301	0,298

$\Delta H = 6D$, where D is the dissociation energy of a diatomic molecule. The discrepancy between the values of ΔH_{sub} in Table VII and the value of $6D$, caused by the long-range interaction, is only slightly larger than the statistical error of the data for inert gas crystals.

From existing information on the parameters of condensed inert gases one can take into account the temperature-dependent variations of the interaction parameters of the interacting atoms. An increase in the temperature of the crystal excites vibrations. Here the effective binding energy per bond, D, must decrease with increasing temperature, while the distance between nearest-neighbor atoms must increase. The latter is reflected in the lower density of the crystal with increased temperature, which changes by 8% on the average as the temperature goes from zero to the melting temperature.

Table VIII lists the reduced parameters of the inert gas crystals. The coincidence of the reduced parameters of the condensed inert gases, and in particular, the reduced melting and boiling temperatures, confirm the validity of the model of atoms with a short range interaction in the analysis of these objects.[1)]

Let us turn to an analysis of the crystal structure of these systems. A condensed system of atoms with a short-range interaction must have a close-packed crystal structure at low temperatures. Two such structures exist,[40–43] the face-centered cubic and hexagonal lattices. In each of them an atom has 12 nearest neighbors. All inert gas crystals have the face-centered cubic structure.

Here we give the small amount of information about these lattices[40–43] that will be required in the subsequent discussion. With a the distance between two nearest neighbors, one can describe a face-centered lattice as two interpenetrating rectangular lattices. The atoms are situated on parallel planes and form a square net on them with a side of length a. The distance between the planes is $a/\sqrt{2}$. A hexagonal lattice also can be constructed by placing the atoms on parallel planes that are spaced a distance $a\sqrt{2/3}$ part. On each plane the atoms are arranged in parallel lines so that the distance between the atoms in a single line is a and the distance between lines is $a\sqrt{3}/2$.

Consequently, the density of atoms in each close-packed lattice is $\sqrt{2}/a^3$. We shall next consider another structure, the body-centered cubic lattice. Each atom in it

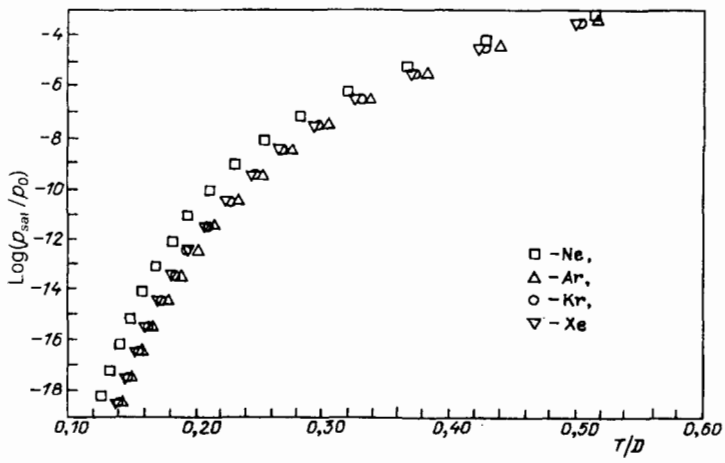

FIG. 8. Temperature dependence of the saturation vapor pressure of inert gases,[39] plotted in dimensionless coordinates.

TABLE VII. Parameters of condensed state of inert gases.[9,38,40]

	Ne	Ar	Kr	Xe
Melting temperature, K*)	24,6	83,7	115,8	161,2
Maximum phonon energy $\hbar\omega_D$, meV				
longitudinal	6,8	8,6	6,2	5,4
transverse	4,6	5,9	4,3	3,8
Sublimation energy, meV/atom	20	80	116	170
Nearest-neighbor distance, Å	3,156	3,755	3,992	4,335
Melting temperature T_m, K*	24,6	83,7	115,8	161,2
Crystal density at the melting temperature ρ_s, g/cm^3	1,444	1,623	2,826	3,540
Liquid density at the melting temperature ρ_l, g/cm^3	1,247	1,418	2,441	3,076
Heat of fusion, cal/mole	80	281	391	549
Boiling temperature, T_b, K*	27,07	87,29	119,8	165,0
Density at the boiling temperature, g/cm^3	1,206	1,378	2,413	2,987
Evaporation energy at the boiling temperature ε_{ev}, kcal/mole	0,422	1,558	2,158	3,02

*)At atmospheric pressure.

has eight nearest neighbors, and the lattice can be obtained from two interpenetrating rectangular lattices. On each plane of the body-centered cubic lattice there is a square array of atoms with a side $2a/\sqrt{3}$, with the distance $a/\sqrt{3}$ between neighboring planes, so that the density of atoms in the body-centered cubic lattice is $3\sqrt{3}/4a^3$, which is 8% lower than that in the lattice with close packing.

Let us analyze the structure of crystals of inert gases. There are two structures with close packing (Fig. 9), in which each atom has 12 nearest neighbors. One of these is the hexagonal and the other is the cubic lattice with the face-centered structure.

In order to understand the relation between the two close-packed structures and the differences between them, we build them up in an identical way. To do so we arrange the atoms, which are assumed to be balls of radius a, on the xy plane so that these balls are laid out in lines parallel to the x axis. Then these lines are placed at a distance $a\sqrt{3}/2$ apart and the centers of the balls of each succeeding line are shifted along the x axis by a distance $\pm a/2$ relative to the centers of the balls of the previous line.

We construct the next plane of balls and move it a distance $a/\sqrt{2/3}$ along the z axis so that the balls of the following plane fall into the hollows between the balls of the previous plane. To do so we shift the upper plane relative to the lower plane by a distance $a/\sqrt{3}$. So far, this construction applies both to the face-centered cubic lattice and to the hexagonal lattice. The third plane can be constructed so that the balls fall into the hollows of the previous plane in two distinct ways. If we displace the plane along the y axis by a distance $+a/\sqrt{3}$, we obtain the face-centered cubic structure, and if we shift it a distance $-a/\sqrt{3}$, we get the hexagonal structure.

The arrangement of nearest neighbors is different for the two structures. It is possible to have both structures in a single crystal, as shown, for example, in Fig. 10. In this case the crystal is made up of individual planes on which the atoms are situated, and starting with a particular plane the direction of the displacement of the plane changes. Then, if the structure of the system is characterized by the arrangement of the nearest neighbors, the atoms of the lowest layers of the crystal shown in the figure belong to the face-centered cubic lattice and the upper atoms belong to the hexagonal lattice, while the atoms of the transitional layer belong to both. Here it is possible to go from one structure to the other not only at the plane z = const, but at any of the 12 symme-

TABLE VIII. Reduced parameters of the condensed state of inert gases.

	Ne	Ar	Kr	Xe	Average
$\delta H_{sub}/D$	5,4	6,6	6,7	7,1	6,4 ± 0,7
T_m/D	0,57	0,59	0,58	0,58	0,58 ± 0,01
T_b/D	0,63	0,62	0,60	0,59	0,61 ± 0,02
ρ_s/ρ_0	0,90	0,92	0,93	0,95	0,92 ± 0,02
$\varepsilon_{ev}/6D$	0,825	0,923	0,907	0,910	0,89 ± 0,04

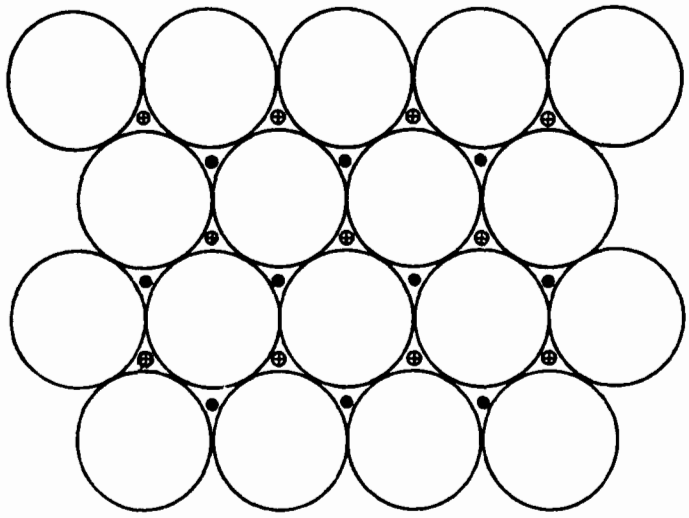

FIG. 9. Close-packed structures intersected by one of the symmetry planes. The atoms are replaced by balls of radius a. The crosses indicate the positions of the centers of the atoms on the lower plane, displaced from the sectioning plane by a distance $a\sqrt{2/3}$. The centers of the atoms on the upper plane, the latter also parallel to the sectioning plane and displaced from it by a distance $a\sqrt{2/3}$ are indicated by open circles for the hexagonal structure and by the points for the face-centered cubic structure of the crystal lattice.

try planes of the structure.

Another conclusion can be drawn from the above discussion. The transformation from one structure to the other requires displacement of individual layers of atoms. It is clear that for a solid system this operation must require an enormous activation energy, proportional to the number of atoms in a layer. Therefore, the actual transformation from one structure to the other is possible only when there is a high concentration of vacancies and apparently occurs either in the liquid state or in the solid phase with a nonequilibrium concentration of vacancies. Therefore, in the analysis of the structure of a crystal or a cluster in the solid state, consisting of atoms with a short range interaction it would be incorrect to draw conclusions concerning the structure (hexagonal of face-centered cubic) only from considerations of the energy of the system at a given temperature. The type of structure also depends on the way it is generated.

In a crystal consisting of atoms or molecules with a short range interaction it is thus possible to obtain either of the close-packed structures, and by an appropriate method obtain a crystal containing both structures. As an example, one may cite the experimental results of Ichihashi *et al.*[45]

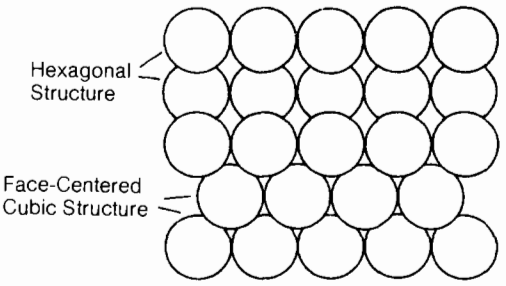

FIG. 10. The transition between the hexagonal and the face-centered cubic structures in a crystal. The crystal is cut by a plane that is perpendicular to the plane of the preceding figure and intersects the latter plane along the line Ox. The sketch shows the cross sections of the atoms—the balls—whose centers lie on or below the sectioning plane.

where thin films of C_{60} were produced by deposition on alkali halide crystals (KCl, KBr, NaCl). An electron microscope (TEM) analysis showed that both structures, the hexagonal and the face-centered cubic, occurred in the films that were formed. The C_{60} clusters are closed molecules whose atoms lie on the surface of a sphere. These molecules interact through the atoms located at the regions of contact of the molecules. Consequently, one can apply to the systems composed of C_{60} clusters all the conclusions regarding a system of atoms with a short range interaction.

Let us clarify the role of the long-range interaction. For simplicity we shall consider only the popular Lennard–Jones interaction potential between the atoms

$$U(r) = D\left[(a/r)^{12} - 2(a/r)^{6}\right], \tag{22}$$

where r is the distance between the atoms. It will be assumed that this potential also acts between distant atoms. Then, according to the calculations in the monograph of Kittel,[40] we find that the energy of sublimation of the crystal with the close-packed structure is equal to $8.61D$. For the hexagonal lattice this is higher by 0.01% than for the face-centered cubic lattice; that is, the sublimation energies of the two structure are essentially identical, and a small perturbation can change the optimum crystal structure.

The main difference from a crystal with a short range interaction between the atoms is that the long-range interaction produces stress in the crystal. The nearest-neighbor distance is different from that in a diatomic molecule, and in the case of the Lennard–Jones potential, it is less than in a diatomic molecule by about 3%.

From this analysis it follows that the long-range interaction in a crystal can be of fundamental importance in the selection of the optimum crystal structure. However, for real inert gas crystals, according to their energies of sublimation, these crystals are better described by a short-range interaction between atoms than by the Lennard–Jones model. Apparently the same can be said also about the distances between atoms in the crystal. Second, a comparison of the sublimation energies listed in Tables VII and VIII indicates that the long-range interaction contributes considerably less

to the sublimation energy than is given by the Lennard-Jones potential. Since in this case the contribution of the long-range interaction is relatively small, we can neglect it in analyzing the various properties of these condensed systems. This conclusion is supported by the fact that the scaling laws for the various parameters of the inert gas crystals are obeyed when these parameters are constructed as combinations of two parameters of the diatomic inert gas molecules: a, the equilibrium internuclear distance, and D the depth of the well in the interaction potential.

The advantage of such a system of atoms with a short range interaction is that the interaction between nearest neighbors does not depend on other bonds. Consequently, one can use such a system as a convenient model in other problems. This model is useful, for example, in the study of the behavior of vacancies in a condensed system of this kind. The pair-wise nature of the interaction gives simple relations for the interaction potential of the vacancies and makes it possible to analyze the processes of joining of vacancies, the way in which the energy of a vacancy changes as it approaches the surface, temperature effects, etc.

3.2. Surface energy of a condensed system

We define the surface energy of a condensed system of atoms as the energy taken up in the formation of a surface when the system is cut into pieces. First we consider an inert gas crystal with a face-centered cubic lattice. We make a cut along a plane parallel to a layer of atoms so that in each of the layers the atoms form a square net with a square side a. Then each atom of the surface layer has eight nearest neighbors and each atom of the next layer has 12 nearest neighbors. In this way, the energy required to form a unit area of the surface (or the energy released in joining the surfaces) is

$$\varepsilon_{sur} = 2D/a^2. \tag{23a}$$

We then make a cut along another plane in which there are six nearest neighbors (this plane is at an angle of 45° to the previous plane). On this plane the atoms are arranged along lines spaced apart by $a\sqrt{3}/2$, and the distance between the atoms in a line is a. The number of atoms per unit area is therefore $2/a^2\sqrt{3}$. Each atom of the surface layer has nine nearest neighbors, and the next layer farther in has 12 nearest neighbors. Hence we find that the specific surface energy is

$$\varepsilon_{sur} = \sqrt{3}D/a^2, \tag{23b}$$

which is slightly lower than that given by formula (23a).

Let us rewrite formulas (23) in another form, introducing the sublimation energy per atom $\Delta H = 6D$ and the density of atoms in the crystal as $N = \sqrt{2}/a^3$. We obtain

$$\varepsilon_{sur} = (0{,}25 \pm 0{,}02)\Delta H \cdot N^{2/3}. \tag{24}$$

It should be mentioned that these expressions refer to the crystal at zero temperature.

We now consider a disorder-type model of the surface of the condensed system, in which the atoms are randomly distributed over the surface of the system, with close-packing of the atoms and for an arbitrary temperature. It will be assumed that the concentration of vacancies inside the crystal is relatively low so that they can be neglected. We shall then construct the surface of the crystal using a filled planar layer with the atoms on it arranged randomly according to statistical rules. As we have seen, the surface energy of a crystal depends somewhat on which symmetry plane of the crystal is chosen as the surface. We shall do this for the two possible variants.

We assume that the surface layer of atoms is a square net with a distance a between neighboring atoms. Then an atom located in the next surface layer can have from four to eight nearest neighbors. The probability P_m that it has m neighbors is given by the Boltzmann formula

$$P_m = g_m \exp(\varepsilon_m/T)\Big(\sum_m g_m \exp(\varepsilon_m/T)\Big)^{-1}, \tag{25}$$

where $\varepsilon_m = mD$ is the energy of binding to the surface of an atom having m neighbors, and $g_m = C_4^{m-4}$ is the statistical weight of this state (the number of combinations of m with $m-4$). Here, $g_4 = g_8 = 1$, $g_5 = g_7 = 4$, $g_6 = 6$.

Using formula (25), we determine the average energy expended in the evaporation of a single atom. We have

$$\varepsilon_{ev} = \sum_m mDP_m p_m \Big(\sum_m P_m p_m\Big)^{-1}, \tag{26}$$

where p_m is the probability of evaporation of an atom with m nearest neighbors. Obviously, this probability is

$$p_m \sim g_m \exp(-\varepsilon_m/T).$$

Consequently, we obtain

$$\varepsilon_{ev} = \sum_m mg_m^2 \Big(\sum_m g_m^2\Big)^{-1}$$

and since $g_m = g_{12-m}$, we obtain

$$\varepsilon_{ev} = 6D. \tag{27}$$

Now we shall examine how the specific surface energy depends on the temperature. We note that the vacancy concentration within the crystal is low. Therefore, when the surfaces of the crystal are joined together the vacancies disappear from the interface. It follows that the specific surface energy increases with the temperature.

The dimensionless surface energy of a crystal is

$$a^2\varepsilon_{sur}/D = \sum_m \big[6 - (m/2)\big] P_m \Big(\sum_m P_m\Big)^{-1}, \tag{28}$$

where P_m is the probability that a surface atom has m nearest neighbors. At zero temperature we have $P_m = \delta_{m8}$, so that $\varepsilon_{sur} = 2D/a^2$. For a finite temperature we have

$$a^2\varepsilon_{sur}D^{-1} = \frac{2(1+2X)}{1+X}, \tag{29}$$

where $X = \exp(-D/T)$. As can be seen, in this model the specific surface energy varies from $2D/a^2$ at zero temperature to $3D/a^2$ at infinite temperature. At the melting temperature ($T_m = 0.58\ D$) the value is $2.3D/a^2$.

Now let us go through the same operation for the case where the plane is the other symmetry plane of the crystal. Joining the nearest atoms in this plane, we obtain a net of equilateral triangles with a side a—the nearest-neighbor distance. In this case the number of nearest neighbors of a surface atom can vary from three to nine, and the statistical weight for the state with a given number of nearest neighbors is the number of combinations C_6^{9-m}. By virtue of symmetry

($g_m = g_{12-m}$), we find, as previously, that the average energy of an evaporating atom is $\varepsilon_{ev} = 6D$. The specific surface energy of the crystal is

$$\varepsilon_{sur} = 2D(a^2\sqrt{3})^{-1} \sum_m \left(6 - \frac{m}{2}\right) C_6^{9-m} X^{9-m} \cdot \left(\sum_m C_6^{9-m} X^{9-m}\right)^{-1} = \frac{D\sqrt{3}}{a^2} \frac{1+3X}{1+X}. \quad (30)$$

At the melting temperature this formula gives

$$\varepsilon_{sur} = 2{,}3\, D/a^2, \quad (31)$$

which essentially coincides with the case where the surface of the crystal was the other symmetry plane.

The energy per bond falls off with increasing temperature because of the excitation of atomic vibrations. Using the measured heats of evaporation for the condensed inert gases, we can determine the amount of this variation. Actually, in the disorder model, the energy expended in removing one atom from the surface is $6D$ (formula (27)). Table VIII gives the reduced values of this quantity, referred to the boiling temperature. A statistical analysis of the parameters of the different inert gases shows that the ratio of the energy required to break one bond at the boiling temperature to that at zero temperature is 0.89 ± 0.04.

The excitation of phonons also increases the distance between nearest neighbors. This results in a decrease in the density of the crystal with increasing temperature. Since the concentration of vacancies in the crystal is relatively low, the change in the density of the crystal with temperature is ultimately due to this effect. The corresponding data are shown in Table VII. A statistical analysis of the data for the different inert gases gives a value of 0.94 ± 0.02 for the ratio of the density at the melting temperature to the density at zero temperature.

Now let us determine the specific surface energy at the melting temperature. For this purpose we use formula (31), taking into account the variation of the energy for breaking of a bond and the variation in the nearest-neighbor distance due to the excitation of phonons. We find

$$\varepsilon_{sur} = (1{,}95 \pm 0{,}13)\, D/a^2, \quad (32)$$

where the parameters D and a refer to zero temperature. As can be seen, the ratio of the surface energy at the melting temperature to that at zero temperature is 1.05 ± 0.15; that is, within the error, the specific surface energy is independent of the temperature. This analysis applies to the crystalline state of a system in which the vacancy concentration is low.

Let us rewrite formula (32), introducing the sublimation energy ΔH and the density of atoms in the system $N = \sqrt{2}/a^3$. In the new variables formula (32) takes the form

$$\varepsilon_{sur} = (0{,}23 \pm 0{,}02)\, \Delta H \cdot N^{2/3}. \quad (33)$$

These results pertain to a close packed structure. It is interesting to compare them with the results of the disorder model, which takes into account the pairwise interaction between the atoms randomly distributed in the system. To calculate the surface energy in this case we cut the element of the solid into two parts, such that each side of the cut forms a surface of area S. We assume that the nature of the interaction between atoms on the surface is the same as in the bulk. Assuming that the arrangement of the atoms is random, we find that each of the surfaces that have been formed contains $SN^{2/3}$ atoms, for which half of the bonds are broken. The energy expended in each surface atom is $\Delta H/2$, and the total energy expended in the formation of the surface is $SN^{2/3}\Delta H/2$. Dividing this energy by the area of the surface that was formed we obtain for the specific surface energy of the system at zero temperature

$$\varepsilon_{sur} = \Delta H \cdot N^{2/3}/4. \quad (34)$$

As can be seen, formulas (33) and (34) coincide within the limits of their accuracy.

3.3. Surface tension of liquids

The relative simplicity of a bound system of a large number of atoms with a pairwise interaction allows us to use it as a model in the investigation of various properties of condensed systems. This possibility will be demonstrated by the examples of the surface tension of solids and liquids.

The surface tension is defined as[44-46]

$$\alpha = \int \left(p_n(x) - p_\tau(x)\right) dx, \quad (35)$$

where $p_n(x)$ and $p_\tau(x)$ are the normal and tangential components of the pressure, the direction of x is perpendicular to the phase boundary, and the integration is carried out over the transition region.

The value of the surface tension is identical to the specific surface energy at zero temperature when there are no vacancies in the system. Thus, the surface tension at zero temperature is given by formula (23). Accordingly, at other temperatures its relation to the parameters of the problem can be given in the form

$$\varepsilon_{sur} = C\, \Delta H \cdot N^{2/3}. \quad (36)$$

Formula (36) can be used to analyze the information relating to the surface tension of liquids. We shall first analyze the data for the surface tension of condensed inert gases. Table IX lists values of the surface tension α_0 of condensed inert gases at the melting temperature, and the values of the coefficient C in formula (36). Figure 11 shows the reduced surface tension α/α_0 as a function of the reduced temperature T/T_m. As can be seen, the scaling is well satisfied. With this result taken into account, Fig. 12 shows the dependence of the reduced surface tension on the reduced temperature, where the dimensionless parameters are constructed from the parameters of the diatomic molecule. Specifically, the dimensionless temperature and surface tension have the form T/D and $\alpha R_e^2/D$, where R_e and D are the equilibrium internuclear distance and the dissociation energy of the diatomic molecule. The experimental data from the review of Baĭdakov[37] were used in Table IX and Figs. 11 and 12.

These results can be used as model results for a wide class of different materials and for non-pairwise interactions between the atoms and molecules. However, for such systems it is still necessary that the nature of the interaction between the atoms or molecules at the surface of the con-

TABLE IX. Surface tension of liquid inert gases at the melting temperature.

	Ne	Ar	Kr	Xe
α_0, ergs/cm^2	5,65	13,55	16,33	18,83
C	0,121	0,130	0,126	0,129
$\alpha_0 R_e^2/D$	0,91	0,98	0,95	0,93

densed system be the same at that in the bulk. Of course, the accuracy of the results will be lower, and in order to understand what the error is, Table X gives the values of the surface tension for metals of the first and second groups at the melting temperature.[48–52] These values are compared with those corresponding to the model of a pair-wise interactions between the atoms, given at the melting temperature (Table IX) by the formula

$$\alpha_m^0 = \Delta H \cdot N^{2/3}/8. \tag{37}$$

A statistical analysis of the data of Table X yields for the ratio α/α_0 the value $10^{0.08 \pm 0.17}$. This means that formula (37) gives the surface tension of metals with an accuracy of about 50%.

Let us make another comment of fundamental importance. The specific surface energy and the surface tension have, generally speaking, distinct meanings. The specific surface energy is the specific energy which is expended in the formation of the surface. The surface tension is the force that acts on a unit length of a contour of a liquid and tends to decrease the enclosed surface area to a minimum under the given conditions. At zero temperature these values are identical for a continuous medium and, in particular, for the condensed systems of atoms studied here. For the liquid state of the system, where the concentration of vacancies in the bulk is appreciable, these quantities are different.

4. LARGE CLUSTERS

4.1. The structure of large clusters

Large clusters are understood to be clusters that contain at least tens of atoms or molecules. These clusters are not macroscopic particles, but constitute a transition state between macroscopic and atomic systems. In the last decade large clusters have been the object of exhaustive investigations (see, e.g., Refs. 53–57), and a great deal of information has been accumulated concerning their properties and behavior in physical systems. Below, a brief review is presented concerning the structure of large clusters.

The structure of large clusters is governed by the nature of the interactions of the atoms or molecules forming the clusters. Therefore, in the analysis of the structure of large clusters we examine individual groups of clusters in which the nature of the interactions between the atoms is the same, and which are described by the corresponding models. The structure of clusters consisting of atoms of the alkali metals have been studied in detail. Such clusters are well described by the jellium model,[58,59] which has been subjected to a series of experimental investigations.[60–67] The main idea of this model is popular in plasma physics—positive changes are uniformly spread out over a volume, which in this case is a sphere of finite radius. Then the valence electrons determine the state of the cluster.

The state of each electron in the system, as in an atom, is characterized by four quantum numbers, the principal quantum number n, the orbital angular momentum l, the projection m of the orbital angular momentum and the projection σ of the electron spin. Because of the degeneracy with respect to the projection of the angular momentum and of the spin, the state of the electron in this model is described by two quantum numbers n and l, as in the atom. However, unlike in the atom, there is no requirement to limit the value of l for a given value of the principal quantum number n.

Thus, if we assume, as in the atom, that the quantum numbers n and l are integral (with $n > 1$ and $l > 0$) we can arrange the electrons into shells, using the same notation as

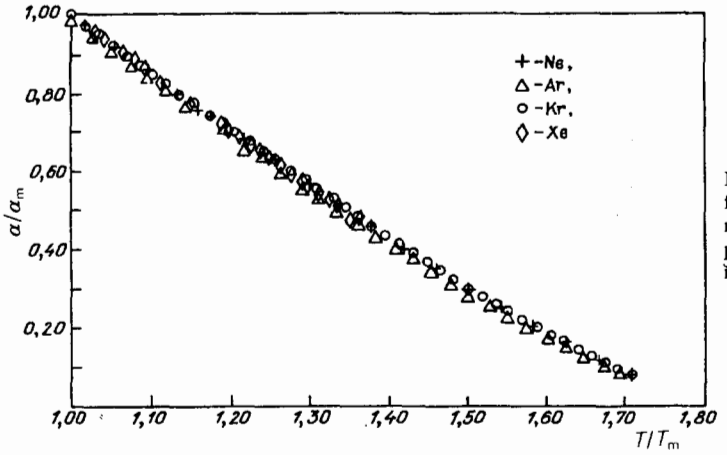

FIG. 11. Ratio of the surface tension of liquid inert gases to their surface tension at the melting temperature, plotted as a function of the reduced temperature (the ratio of the temperature to the melting temperature). The data are those recommended from the analysis of Baĭdakov.[37]

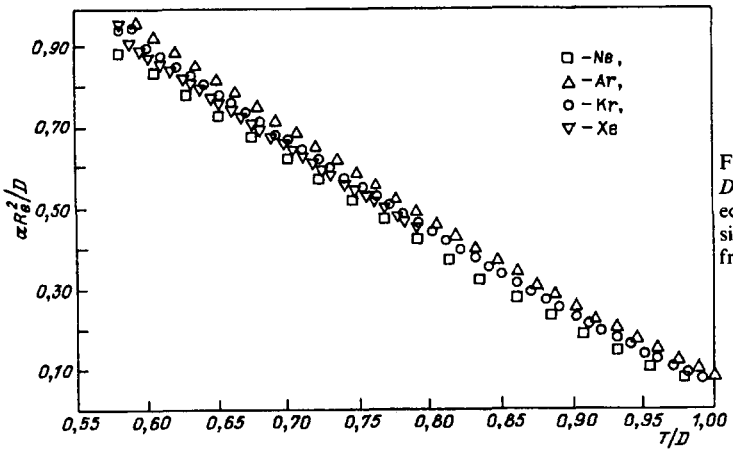

FIG. 12. Surface tension of liquid inert gases in units of D/R_e^2 (where D is the dissociation energy of the diatomic molecule and R_e is its equilibrium internuclear distance, plotted as a function of the dimensionless temperature T/D. The values of the surface tension are taken from the review of Baĭdakov.[37]

for the atom. Naturally, the lowest is the $1s$ shell (2 electrons) and then comes the $1p$ shell (6 electrons). Starting with some value of the angular momentum, the $2s$ shell becomes energetically more favorable than the $1l$ shell. Figure 13 shows the sequence of the filling of the shells within the framework of the jellium model, constructed according to the experimental results.[62–67] The clusters with filled shells are the most stable, so that the filled shells correspond to magic numbers. It follows from the experimental results that some electron shells of the cluster are filled simultaneously (Fig. 13).

It is an interesting fact that the jellium model works for a finite number of atoms in a cluster. According to the experiments of Martin *et al.*,[66] who studied the structure of the Na_n cluster with $n < 22\,000$, the jellium model works when the number of atoms in a cluster is $n < 1500$. Thereafter, the fundamental factor is the pair interaction between the atoms, and the magic numbers of the cluster correspond to the structure of the icosahedron or the cube octahedron.

The carbon clusters C_{60}, C_{70}, C_{84}, etc. have found great popularity (see, e.g., the reviews in Refs. 68 and 69). The atoms in these clusters form a closed surface similar to the covering of a soccer ball. It is interesting that the cluster Si_{60} has the structure of a pyramid,[70] even though the silicon atom has the same electron structure as carbon.

Since the structure of the cluster is determined by the nature of the interaction between the atoms in it, these structures are as varied as the structures of the crystal lattices. In large clusters the arrangement of the nearest-neighbor atoms is the same as in the corresponding crystal. The surfaces of large clusters containing hundreds or thousands of atoms have surfaces with planar elements. For example, Cleveland and Landman[71] have analyzed the structures of nickel clusters and found that when the number of atoms in a cluster is $n < 2300$, then it is an icosahedron, while for $2300 < n < 17\,000$ it is a dodecahedron. Similar results were obtained previously for a cluster consisting of atoms with a Lennard–Jones potential (see Sec. 4.3).

New possibilities for the formation of clusters, and, consequently new possibilities for magic numbers are obtained when the cluster consists of atoms with different valence electrons or contains atoms of different types. For example, in their investigation of clusters containing silver and gold atoms, the authors of Ref. 72 determined their struc-

TABLE X. Surface tension of liquid metals of the first and second groups at the melting temperature.

Metal	α_m, J/m^2	α_m^0, J/m^2
Li	0,41	0,43
Be	1,14	1,68
Na	0,20	0,19
Mg	0,57	0,38
K	0,109	0,104
Ca	0,42	0,44
Cu	1,30	1,35
Zn	0,77	0,44
Rb	0,088	0,083
Sr	0,35	0,23
Ag	0,94	0,90
Cd	0,56	0,30
Cs	0,069	0,069
Ba	0,27	0,22
Hg	0,474	0,16

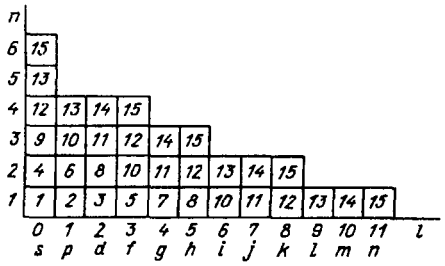

FIG. 13. Sequence of filling the shells of clusters of alkali metals, based on the jellium model and constructed according to the experimental results of Refs. 62–67.

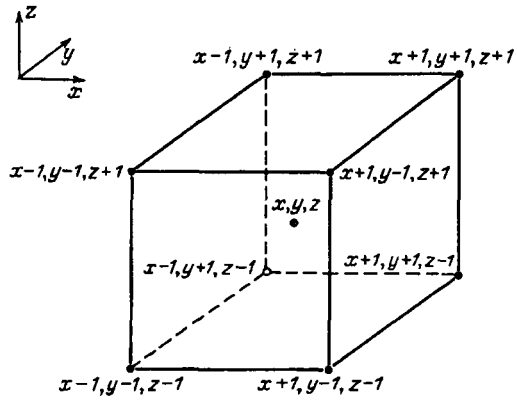

FIG. 14. Coordinates of the nearest neighbors of an atom with the coordinates xyz in a system with the body-centered cubic structure. The spacing between the nearest neighbors in the units used is $\sqrt{3}$. The coordinate system used is in the upper left part of the figure.

ture, which they called supraclusters. In this case, 13 atoms have the structure of an icosahedron and are the central block of a cluster on which clusters of another type are later arranged.

4.2. Structure of large clusters with close packing

The above discussion of the pairwise interaction of atoms is convenient to use for an analysis of the properties of any bound system of atoms. We shall consider larger clusters composed of atoms with a short-range interaction, that is, a system of a finite (but large) number of atoms. To simplify the analysis we shall assign to the cluster one of the previously discussed crystal structures.

Using this tactic in the construction of the cluster, a system of n bound atoms with short-range interaction, we proceed in the following manner. We take a crystal structure as a basis and cut out from the interior an element containing n atoms. This will be called a cluster. The cluster can also be constructed in other ways, selecting the atoms so that they have a given crystal structure. Then we count up the energy of the cluster, which for a short range interaction is equal to the number of bonds in it multiplied by the bond energy of a dimer. Then we change the configuration of the atoms while retaining the chosen crystal lattice. For each configuration of atoms we calculate the corresponding energy. If the temperature is zero, we select that configuration that corresponds to the minimum energy. If the temperature is nonzero, then we consider other configurations with a weak perturbation. These operations are not so arduous, as can be shown. For clusters with face-centered cubic and body-centered cubic lattices containing up to 1000 atoms, the calculations can even be done without a computer.

The operations are partially described in Ref. 73. Here they will be demonstrated with the example of a cluster with a body-centered cubic lattice. We place one of the atoms at the origin of coordinates and choose as the unit of length the length $a/\sqrt{3}$ (where a is the nearest-neighbor distance). Then the nearest neighbors of the atom with the coordinates xyz are eight atoms, whose coordinates are $x \pm 1$, $y \pm 1$, $z \pm 1$ (Fig. 14).[40–43]

The cluster has two types of symmetry. One of them corresponds to the transformations $x \leftrightarrows y \leftrightarrows z$ and the other to the transformations $x \leftrightarrows -x$; $y \leftrightarrows -y$; $z \leftrightarrows -z$. Using this fact, we can divide the cluster into shells so that the coordinates of all the atoms of a given shell can be obtained from the coordinates of one of them by the above transformations. In this way one can thereafter limit the analysis to the position of only one of the atoms of the shell. It is convenient to choose as this atom the one with positive coordinates and with $z \leqslant x \leqslant y$ (the z axis is perpendicular to the plane in which the atoms lie).

Then we count up the number of nearest neighbors of the atoms of the given shell. This allows us to calculate the energy of the cluster with a given number of atoms and specified filled shells. From this we can choose the optimum order in which the shells of the cluster are filled and find the energy of the cluster with a given number of atoms and the binding energy of the cluster of connected atoms. Let us analyze the results so obtained.

It might appear that as new atoms are added to the cluster the latter should grow by filling the shell nearest to the center of the cluster. In a rough approximation this is so, but in a more detailed analysis we find that this principle is frequently violated. Sometimes (i.e., for certain numbers n of atoms in the cluster) the sequence of the filling of the shells of the cluster changes. In other cases it is more favorable for the cluster to grow with the participation of several shells. Then the addition of new atoms to the cluster is accompanied by the growth of the individual shells, which then can be joined to each other.

An illustration of this process is given in Table XI, which shows how a cluster with a body-centered cubic lattice and a large number of atoms grows at the region where the shell-wise manner of cluster growth is violated for the first time. Table XII shows the manner of growth of a cluster with a face-centered cubic structure over a wide range of occupation numbers n. As can be seen, the simultaneous filling of several shells occurs quite frequently.

We shall derive an expression for the parameters of the cluster at zero temperature. In the case considered, where only pair interactions operate, the total energy of a cluster, $E(n)$, is proportional to the number m of bonds in the cluster.

$$E(n) = -mD, \tag{38}$$

where D is the dissociation energy of the dimer. For $n \to \infty$, the number of bonds tends to nk, where $2k$ is the number of nearest neighbors per atom in the given structure of the system. We introduce the surface energy of a cluster as

TABLE XI. The way atoms are attached to a cluster in the region where the shell-wise mode of growth is first violated.

Number of atoms in the cluster	Coordinate of the last atom	Surface energy of the cluster, units of D
16	022	30 (30)*)
17	113	32 (32)
18	202	33 (34)
19	220	35 (36)
20	131	36 (38)
21	222	37 (40)
22	311	37 (42)
23	202**)	39 (44)
24	113	40 (46)
25	220	42 (48)
26	131	43 (50)
27	222	44 (52)
28	313	44 (53)

*)The values in the parentheses correspond to the sequential filling of the shells.
**)The overbar stands for a minus.

$$E_{sur}(n) = nkD + E(n). \quad (39)$$

The binding energy of an attached atom is

$$\varepsilon(n) = E(n-1) - E(n) = kD + E_{sur}(n-1) - E_{sur}(n). \quad (40)$$

By comparing the energy of clusters with the same given number of atoms but with different structures, one can choose the optimum cluster structure. It is clear that this cluster can have only one of the structures with close packing, the hexagonal or the face-centered cubic. Table XIII lists the energy of a cluster with a short range interaction between atoms in different structures for two values of the occupation number. Although the optimum structure of the cluster in both cases is the face-centered cubic structure, the difference from the hexagonal lattice is so small that the inclusion of a small amount of long-range interaction could

TABLE XII. Order of growth of a cluster with face-centered cubic structure.

Filled shells*)	Range of variation of η	Range of variation of the surface energy, units of D
011(1—5)	2 — 13	12 — 42
004 (4)	13 — 19	42 — 54
112(3—5) + 022(5)	19 — 55	54 — 114
013(4—6)	55 — 79	114 — 138
123(3—5) + 222 (6)	79 — 135	138 — 210
033(5)	135 — 147	210 — 222
004(4) + 114(5) + 024(6)	147 — 201	222 — 258
233(3—5) + 224(6)	201 — 249	258 — 330
015(4—6) + 134(5—6) + 125(5—6)	249 — 369	330 — 402
044(5) + 035(6)	369 — 405	402 — 414
006(4) + 116(5) + 026(6)	405 — 459	414 — 450
334(3—5) + 244(5) + 235(5—6) + 145(5—6)	459 — 603	450 — 570
226(5) + 136(6)	603 — 675	570 — 594
055(5) + 046(6)	675 — 711	594 — 606
017(4—6) + 127(5—6) + 037(6)	711 — 807	606 — 654
008(4) + 118(5) + 028(6)	807 — 861	654 — 690
444(3) + 345(4—6) + 255(5) + 336(5) + 246(6) + 156(5—6) + 237(5—6) + 147(6)	861 — 1157	690 — 858
066(5) + 057(6)**)	1157 — 1193	858 — 870
228(5) + 138(6)**)	1193 — 1265	870 —894
455(3—5) + 446(5) + 356 (5—6) + 347(5—6)	1265 — 1409	894 --1014
366(5) + 257(6)	1409 — 1481	1014 — 1038

*)The parentheses indicate the number of nearest neighbors for the atoms of that shell.
**)The individual islands of these shells can be filled in any order.

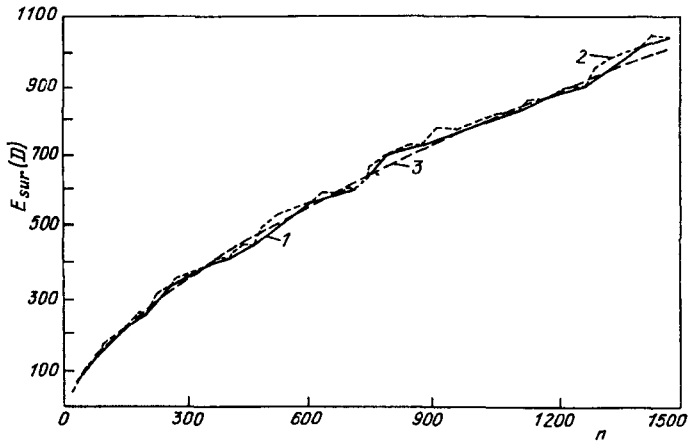

FIG. 15. Surface energy of a cluster with the face-centered cubic lattice structure at zero temperature. Curve *1* takes into account the actual way the cluster grows by filling of the separate islands; curve *2* corresponds to the shell structure of the cluster, and curve *3* represents the approximation of formula (41).

change the optimum structure of the cluster.

The cluster model considered here with a specific crystal structure and pairwise interactions between the atoms makes it possible to understand the various aspects of the physics of large clusters. One question is: at what filling number does the cluster become a macroscopic particle? By definition, a cluster is considered a macroscopic particle if its parameters are monotonic functions of the number of atoms in the cluster. The answer to this question is the following.[73] From the point of view of the energy of an atom bound to the cluster, which is a power-law function of the number of atoms, a cluster containing hundreds of atoms is not a macroscopic particle. The surface energy of a cluster varies approximately as $n^{2/3}$ to an accuracy of a few per cent; that is, it is proportional to the surface area of the cluster. In particular, Fig. 15 shows the variation of the surface energy of a cluster with the face-centered cubic structure in the range of n corresponding to the data of Table XII. Figure 16 shows as a function of the number of atoms in a cluster the variation of the constant of proportionality B in the formula for the surface energy of the cluster

$$E_{sur} = Bn^{2/3}D. \tag{41}$$

This formula was obtained from the data of Table XIII. As is apparent, B is an irregular function of the number of atoms in a cluster. Therefore, the approximation (41) is possible, but with limited accuracy, estimated to be a few per cent.

The possible validity of such an approximation can be explained by the following argument. The surface energy of a cluster containing tens or hundreds of atoms comes from many shells and most of the atoms of a cluster containing hundreds of atoms. At the same time, the binding energy of an attached atom depends on which shell it belongs to, that is, how many nearest neighbors it has. In this way, the energy of an attached atom is quantized.

However, this same situation corresponds to a cluster with any number of atoms. One can expect that this is a zero-temperature effect. An increase in the temperature smooths out the variation of the binding energy of an atom attached to a cluster as a function of the number of atoms in the cluster. Estimates[73] show that this smoothing actually occurs, although even for clusters with $n \sim 100$–1000 at temperatures up to the melting point of the crystal the binding energy of an attached atom is not a monotonic function of n and deviates from $-\mathrm{d}E(n)/\mathrm{d}n$, which applies to a macroscopic cluster (E is the total energy of a cluster).

Thus, a large cluster consisting of atoms with a pairwise interaction, i.e., a bound system of a large number of atoms with a pairwise interaction, can be analyzed from the point of view of the energy parameters of the system. Choosing a

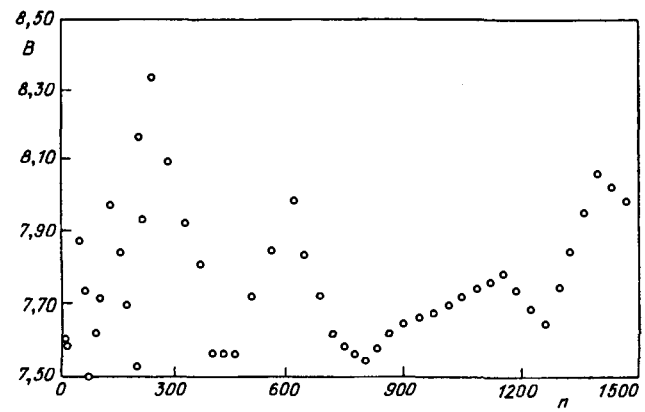

FIG. 16. Dependence on the number of atoms in a cluster of the numerical coefficient in formula (41) equal to $B = E_{sur}/Dn^{2/3}$.

TABLE XIII. Energies of clusters with different structures, in units of D.

Cluster structure	$n=257$	$n=349$
Face-centered cubic	−1208	−1691
Body-centered cubic	−808	−1144
Hexagonal	−1204	−1688

particular type of symmetry for the cluster, one can calculate the total energy of the system for various configurations of the atoms. It is thereby possible to find as a function of the number of atoms in the cluster the optimum symmetry and configuration of the atoms at zero temperature in a cluster that contains a given number of atoms. The same operations can be carried out for finite, relatively low temperatures for which the number of vacancies in the filled shells is relatively small. It should be emphasized that these results are very intuitive because their derivation does not depend on tedious and difficult mathematical methods even when the system contains hundreds of atoms.

4.3. Clusters with the Lennard–Jones Interaction

A cluster in which the atoms interact through the Lennard–Jones potential, formula (22), have been studied very thoroughly (see, e.g., Refs. 74–85). Below, those results will be analyzed from two points of view. First, the results provide a deeper understanding of the structure of large clusters and permit a choice of the optimum approach for the analysis of their properties. Second, it is convenient on the basis of these results to analyze the advantages and the drawbacks of this method of constructing clusters consisting of atoms with a short range interaction.

The Lennard–Jones potential for the interaction between atoms separated by a distance R is given by formula (22)

$$U(R)=D[(a/R)^{12}-2(a/R)^{6}], \tag{42}$$

where the distance a between the atoms corresponds to the minimum of the interaction potential, which is equal to D at that distance. Let us construct a cluster consisting of atoms with this interaction. The difference between it and a cluster with a short-range interaction is that the long-range interaction between atoms that are not nearest neighbors can create stress in the cluster. This causes a shift of the distance between neighboring atoms from the interatomic distance in the diatomic molecule.

For this same reason a cluster with a long-range interaction between the atoms admits of new structures, not available to a cluster with a short-range interaction between atoms. Within this model the distances between nearest neighbors atoms were strictly specified, and not subject to small changes. However, if it is assumed that the distances between nearest neighbors atoms are close to some value, but can vary over a certain range near this value, then new structures can be obtained. The most important of these structures is the icosahedron.[84]

Let us discuss the general methods of the theoretical analysis of the Lennard–Jones cluster, which has been the subject of many investigations.[74–89] It might appear that to find the optimum configuration of the atoms in a cluster it would be sufficient to choose some appropriate configuration and then adjust the positions of the atoms until the energy of the cluster becomes a minimum. However, as it turns out, this method does not work. Even for a Lennard–Jones cluster containing 13 atoms there are at least 988 local energy minima,[74,75] and one can expect that this number increases rapidly with the number of atoms in the cluster. Therefore, other approaches are used, based on an analysis of the appropriate structures of the cluster. Such an analysis is particularly suitable for clusters with filled shells.

We shall carry out this analysis for clusters containing 13 atoms. In this case a cluster with a close packed structure has a cube octahedron structure (Fig. 17) and a filled first shell. The number of bonds is 36, so that the total energy of the crystal in terms of the short-range interaction between atoms is $36D$, while for the Lennard–Jones interaction including the long-range interaction and a small reduction of the interatomic distance on account of it, the energy is $40.48D$.

In the case of the icosahedral structure (Fig. 18) the number of bonds for an interatomic distance close to the

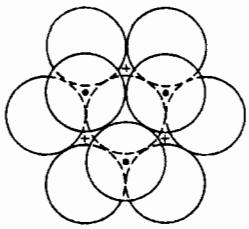

FIG. 17. Thirteen-atom cluster with the structure of a cube octahedron. It has three atoms each in the upper and lower layers and seven atoms in the middle layer. The positions of the center of the atoms of the lower layer are indicated. The crosses indicate the structure of the face-centered cubic lattice and the filled circles indicate the hexagonal structure.

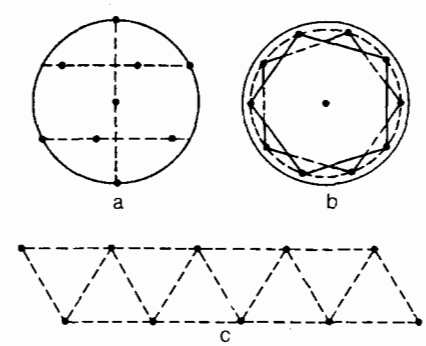

FIG. 18. Thirteen-atom cluster with the icosahedral structure. The filled circles indicate the positions of the centers of the atoms. a) Side view; b) top view; c) an unrolled cylinder with inscribed pentagons.

TABLE XIV. Number n_i of bonds in a cluster with $n = 13$ atoms and the structure of an icosahedron for a given distance R_i between atoms.

R_i/a	0,964	1,014	1,640	1,928
n_i	12	30	30	6

equilibrium distance in the molecule is 42 (Table XIV). Therefore, the energy of this structure, $44.3D$, is lower than for the cube octahedron. The icosahedral structure is thus optimum at zero temperature for a cluster with the Lennard–Jones potential. Table XIV gives the parameters of an icosahedral cluster containing 13 atoms.

It is clear that the icosahedral and cube octahedral structure are optimum for a cluster in which the short-range interaction is dominant. In any case, this conclusion refers to clusters with closed shell. Here the surface of the icosahedron consists of 20 equilateral triangles, with the number n of atoms in it given by the formula[86]

$$n = (10m^3/3) + 5m^2 + (11m/3) + 1, \qquad (43)$$

when the mth shell is full. The surface of a cube octahedron consists of eight equilateral triangles and six squares. It has the same magic numbers, i.e., the numbers of atoms in the filled shells as the icosahedron, but its volume is somewhat greater. Let us consider, for example, a cluster consisting of 13 atoms. For both structures the centers of the atoms are on a sphere whose center is the central atom. The radius of this sphere in the case of a cube octahedron is 3.7% larger (and the enclosed volume is 11.7% greater) than for the icosahedron.

A comparison of these structures shows[78,80–82,85] that when the number of atoms in a cluster is $n < 1000$ the favored structure is the icosahedron. Thereafter, over a large range of n the energies of these structures are nearly the same, and for very large n the close packed structure is the optimum one. Table XV shows the binding energies of the atoms in a cluster for filled shells in the icosahedral and cube octahedral structures.[82] The transition from the icosahedral structure to the cube octahedral structure according to the data of this investigation occurs in the 14th shell, when the number of atoms is $n = 10\,179$. However, the exact size of the cluster when the transformation occurs from one structure to the other has no fundamental significance. In fact, the difference in energy between these structures for $n \sim 1000$ is about 1%, so that the sign of this difference can be changed with a small change in the potential. This is all the more true, since in the analysis of the parameters of the inert gas crystals it has been shown that they are better described in terms of a short-range interaction potential between the atoms than by the Lennard–Jones potential.

Experimental analyses of the structure of large inert gas clusters employ the method of electron diffraction by clusters formed in the expansion of a gas in the space beyond the nozzle. Investigations of argon clusters[83,84] have shown that they are icosahedral for $50 < n < 800$, while for $n > 800$ the observed electron resonances are better described by the face-centered cubic structure. According to the data of Ref. 85, clusters of argon, krypton, and xenon with $n = 100$–300 have the icosahedral structure. Measurements for large argon clusters have shown[78] that for $n < 1500$ they have the icosahedral structure, while in the range $n = 1500$–3500 there is a smooth transformation to the face-centered cubic structure. The experiments thus confirm that inert gas clusters containing tens and hundreds of atoms have the icosahedral structure, while if the cluster contains thousands of atoms the face-centered cubic lattice is the preferred one.

The question arises as to how sensitive the optimum structure is to the shape of the interaction potential between the atoms. To address this question, Table XVI presents the values of the total binding energy in a cluster containing 13 atoms with the icosahedral structure (E_i) and the cube octahedral structure (E_c), where the interaction potential between the atoms has the form

$$U(R) = D\left[\frac{(a/R)^l}{l} - \frac{(a/R)^k}{k}\right]\left(\frac{1}{k} - \frac{1}{l}\right)^{-1} \qquad (44)$$

(the notation is the same as in formula (22)). The calculations pertain to different values of the parameters l and k. It follows from the data in the table that the choice of optimum

TABLE XV. Total binding energy of atoms in a cluster for the cube octahedron structure, E_c, and the icosahedral structure, E_i, with the Lennard–Jones potential between the atoms.[82]

Shell number	Number of atoms, n	Binding energy, units of D	
		E_i	E_c
1	13	44,33	40,88
2	55	279,2	268,3
3	147	876,5	854,4
4	309	2007	1972
5	561	3842	3792
6	923	6553	6488
7	1415	10309	10232
8	2057	15282	15196
9	2869	21641	21552
10	3871	29559	29473
11	5083	39205	39130

TABLE XVI. Binding energy of atoms in a cluster with $n = 13$.

	k,l = 4—8	6—12	8—12	8—16	12—18
E_i / D	50,23	44,33	42,45	43,60	39,56
E_c/D	47,27	40,80	38,79	38,10	36,62

structure of the filled shells of the cluster is not very sensitive to the form of the interaction potential.

Figure 19 shows the binding energies of a surface atom in a cluster for the case of the Lennard–Jones interaction between the atoms as the second and third shells of the icosahedron are filled.[77] In a rough approximation the following picture is obtained for a cluster with close packing. The binding energy does not change as one of the shells is filled or it changes with a certain periodicity. Moreover, there are features that are apparently related to the nature of the interatomic interaction. In the filling of the third atomic shell the clusters with $n = 70$, 79, and 135 stand out. These values must be the magic numbers of the cluster, i.e., in the gas where the clusters are formed these clusters must be somewhat more numerous than for adjacent values of n. For comparison, the magic numbers of the Xe_n^+ clusters in this region of n are 71, 87, and 141 (Ref. 87).

A brief analysis of the experiments on charge clusters A_n^+ ($A \equiv Ne, Ar, Kr, Xe$)[87–96] leads to the following conclusions. The magic numbers of clusters of different kinds frequently do not coincide, which indicates the sensitivity of the structure of the cluster with unfilled shells and the nature of the interaction in it. The same magic numbers are not always obtained in different experiments with the same element. This is evidence for the role of the conditions under which the clusters are formed. In addition, all the experiments corroborate the fact that the filled icosahedral structure is the most stable. The magic numbers observed in various experiments for the different elements correspond to this situation. These numbers are 13, 55, 147, 309, 561, and 923.[2)] Turning now to the method of constructing clusters with close packing, let us analyze its merits and shortcomings on the basis of the information obtained for the Lennard–Jones potential. As has been seen, the optimum structure of this cluster for not too large values of n is the icosahedron. This structure does not fall into the category of structures with close packing, with elements modeled by hard spheres so that the spacings between neighboring atoms are strictly specified. The icosahedron is modeled by elastic balls and does not have the symmetry of the close packed structures, which has previously helped to simplify the problem. Therefore, one cannot by this method determine the optimum cluster energy at zero temperature.

A virtue of this method is its simplicity, which permits analysis of the clusters with arbitrary (but not too large) values of n. This makes possible an approximate analysis of various properties of a large cluster, particularly with the use of numerical methods.

4.4. Surface energy of clusters

Figure 15 shows the surface energy of a cluster with the face-centered cubic lattice containing a large number n of atoms. This curve refers to zero temperature. As can be seen, the dependence on the number of atoms in the cluster is the same as for a macroscopic cluster, where this energy is proportional to the surface area, i.e., to $n^{2/3}$ (see formula (41)). Figure 16 gives the constants of proportionality in formula (41). The value of B is seen to be a random function of n,

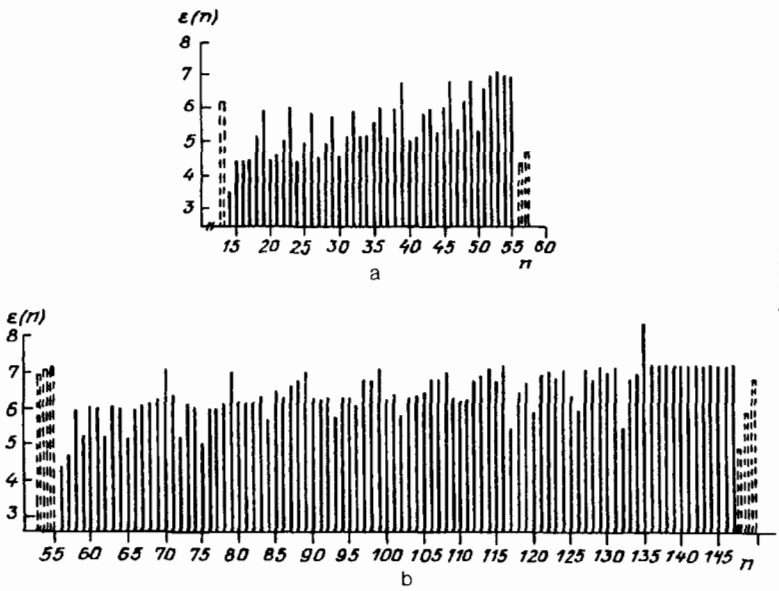

FIG. 19. Binding energy of a surface atom (in units of D) in a Lennard–Jones cluster at zero temperature.[77] a) $n = 13$–55; b) $n = 55$–147.

with oscillations that decrease in amplitude with increasing n. A statistical analysis of the data in Fig. 16 gives

$$B = 7.8 \pm 0.2, \tag{45}$$

and consequently, this quantity within a few per cent can be considered as constant.

If we regard a cluster as a macroscopic particle, we obtain the specific surface energy as

$$\varepsilon_{sur} = E_{sur}/4\pi r^2 = CD/a^2, \tag{46}$$

where $C = A(18\pi)^{1/3}$. Formulas (45) and (46) yield $C = 2.03 \pm 0.05$, which agrees with the expression for the specific surface energy of a crystal, formula (23), within the limits of accuracy of these results.

As the temperature is raised, the surface energy of a cluster increases, since some atoms of the cluster move into shells with a lower atomic binding energy. Because there is a release of surface energy of a cluster when two clusters are joined together, not only is the temperature-dependent variation of the surface energy of the cluster important, but also important is the fact that this quantity depends on the number of atoms in the cluster.

Figure 20 shows the relative temperature-dependent variation of the surface energy for a number of clusters with closed shells. An analysis of these data shows that the temperature dependence of the surface energy of a cluster is an irregular function of the number of atoms in a cluster. It depends, first of all, on the number of atoms in a cluster with binding energies $7D$ and $6D$ in the filled shells of the cluster and the number of atoms with a binding energy $5D$ in the unfilled shells, because the variation in the surface energy of a cluster is mainly related to transitions of the atoms between these shells. Consequently, if two clusters are combined and the excess surface energy is released, then the temperature dependence of this difference in the surface energy can be different depending on the structure of clusters that are joined and the structure of the cluster that is formed.

In a demonstration of this statement, we assume that the temperature dependence of the surface energy for clusters with $n \sim 200$ is the same as that for a cluster with $n = 201$; that for clusters with $n \sim 400$ is the same as that for a cluster with $n = 405$; and that for cluster with $n \sim 800$ is the same as that for a cluster with $n = 791$. We then find that the energy released in the union of clusters with $n \sim 200$ is 18% higher at the melting temperature than at zero temperature, and the energy released in the union of two clusters with $n \sim 400$ is 5% lower at the melting temperature than at zero temperature.

A separate question is that of determining the surface energy of a cluster when there are long-range interactions between the atoms. If the total energy of a cluster is defined according to the formulas (39) and (41)

$$E(n) = An + Bn^{2/3}, \tag{47}$$

the coefficient A is a smooth function of n since the contribution by the long-range interaction to the sublimation energy of a cluster differs from the corresponding quantity for an infinite crystal. It is therefore correct to introduce the surface energy as the part of the energy that is released when two clusters combine into a large cluster. Then the surface energy of a cluster is given by the formula

$$E_{sur} = \frac{3}{2} n \frac{d(E/n)}{dn}. \tag{48}$$

This formula works in a limited range of n. In accordance with this formula, an expression for the surface energy of a cluster is

$$E_{sur} = \gamma \Delta H \cdot n^{2/3}, \tag{49}$$

where $\Delta H = A$ is the sublimation energy per atom of the cluster. This quantity depends on the size of the cluster. For a Lennard–Jones cluster the coefficient of proportionality γ is equal to 1.51 if we use the energy values obtained for clusters with the icosahedral structure with $n < 3000$ (Ref. 78) and $\gamma = 1.43$ if we use the results of a numerical calculation[77] for clusters with $n \leqslant 150$.

5. POROUS SYSTEMS

5.1. Surface energy of dilute porous systems

The results that have been obtained for the surface energy can be used as model results in the analysis of porous materials, made up of small elements. A problem of this type will be analyzed below. A porous material with an internal surface of large specific area has a high surface energy. This energy can be released and transformed into heat as the specific area of the interior surface is reduced. The release of the

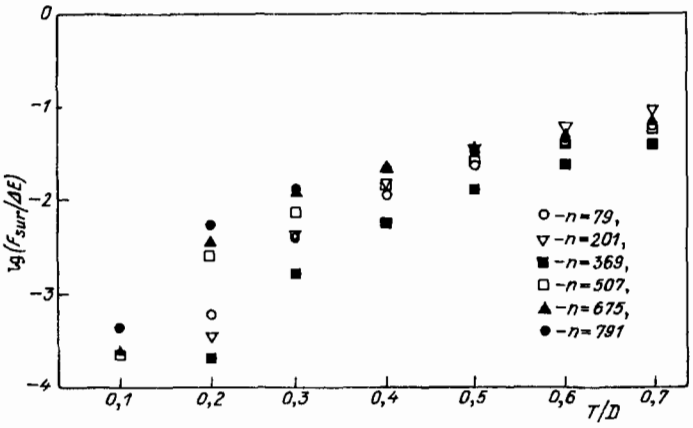

FIG. 20. Temperature dependence of the relative variation in the surface energy of a series of clusters with the face-centered cubic structure and filled shells.

heat increases the temperature of the sample and may accelerate the reduction of the internal surface area of the sample. Under some conditions this can cause a thermal explosion[99] owing to the rapid transformation of surface energy into heat. This process can propagate in porous material in the form of a thermal wave.

Such a process for an aerogel[100,101] and a fractal filament[102,103] has been analyzed by the present author previously.[99] A thermal explosion of an aerogel, caused by the leakage and ignition of methyl alcohol, might have been the cause of the explosion that occurred in 1984 in the Swedish company AEROGLAS,[104] which used to produce silicon dioxide aerogel in large quantities. However, this statement and numerical estimates have provoked disagreement on the part of specialists. Therefore, on the basis of the previously obtained results, we shall analyze the threshold parameters of the process.

The process proceeds in the following way. As the temperature of the structure approaches the melting temperature, the structure decomposes into liquid droplets, which then merge with one another. The energy liberated in this way is transported into the adjacent elements of the construction and cause the latter to melt. The formation of liquid droplets accelerates the process by several orders of magnitude, so that for a thermal wave to travel along a fractal filament it is necessary that only a part of the material become liquid. Otherwise, the characteristic time of heat transfer is less than the time of reduction of the inner surface area, so that the thermal wave cannot propagate along the fractal filament. For an aerogel the conditions are not so stringent, but the temperature at the thermal wave front must be quite high for the reduction of the specific area to occur effectively. Then we require that for the process to proceed the surface energy of a simple system must be sufficient to heat the material to the melting temperature.

The surface tension and the specific surface energy are different characteristics, although they coincide at zero temperature. The surface tension is characterized by a difference in the normal and tangential forces acting on an atom as it moves through the interface. This quantity is sensitive to the formation of vacancies on the surface near the interface, so that it decreases rapidly with increasing temperature, particularly in the liquid state of the material. For a liquid system of atoms with a short range interaction the surface tension at the melting temperature is about half that at zero temperature and falls off rapidly as the temperature is raised above the melting point.

The specific surface energy for a system of atoms with a short range interaction does not change so rapidly with the temperature. Unlike the surface tension, this quantity is not so sensitive to the vacancy concentration at the surface and within the system. For a liquid at the melting temperature it is given by formula (32) and is only slightly lower than the value given by formula (24) at zero temperature. In this analysis formula (32) will be used for the specific surface energy of a simple system.

This formula (32) applies to systems with a short range interaction between the atoms and can be used as a model for other systems. In the latter case the accuracy of the formula is estimated at $\sim 50\%$ on the basis of a comparison of the actual values of the surface tension with those of the model formula.

Let us use formula (32) for an aerogel of silicon dioxide. From the parameters of silicon dioxide ($\Delta H = 133$ kcal/mole and $\rho = 2.1$ g/cm^3)[105] we obtain for the specific source energy of this material $\varepsilon_{sur} = 1.6$ J/m^2. If we assume that the specific heat of silicon is temperature independent, then, using the room temperature value $C_p = 0.75$ J/g·K (Ref. 105), we find that the threshold for this process corresponds to a specific aerogel surface of 800 m^2/g. We recall that this result is accurate to a factor of about 2. The maximum specific area of a silicon dioxide aerogel is about double that of the threshold value. We can therefore expect that existing samples of the aerogel may be explosive materials, although the reliability of this conclusion is limited.

Nonetheless, this result can be used as an estimate for a more accurate determination of the parameters of the thermal explosion of an aerogel. To make such a determination, a piece of the aerogel can be heated and at various sample temperatures one of its elements brought to the melting temperature, by laser irradiation, for example. The sample temperature at which the thermal explosion occurs provides information on its surface energy and thermophysical parameters of the aerogel at high temperatures.

There is another circumstance related to this process. Let us consider an aerogel with the maximum specific internal surface area $S = 1500$ m^2/g (Ref. 106). We analyze this aerogel using the well-known model of a collection of independent balls. Each ball has a radius $r = 0.41$ nm, and since the density of molecules in solid silicon dioxide is $2.1 \cdot 10^{22}$ cm^{-3}, we find that each ball contains approximately 260 molecules. In this way, each ball is a medium-size cluster and not a macroscopic particle. The phase transition to the crystal is of a different nature, and this means that the cluster has a larger specific surface energy than a macroscopic particle.

5.2. Bubbles and the solid-liquid phase transition

It is well known[107] that the solid-liquid phase transition is associated with the formation of vacancies (voids) within the condensed system. These vacancies cause loss of long range order in the system. We shall investigate this problem phenomenologically on the basis of the transition parameters measured for condensed inert gases (Table VII), using the scaling laws, along with the idea of the formation of vacancies in the liquid state of a system with a short range interaction between the atoms.

The concentration of vacancies is very low in the solid state of the system. At the melting temperature, $T_m = 0.58D$, the Boltzmann factor in the probability of the thermally-induced formation of a simple vacancy is $\exp(-12D/T) = 1 \cdot 10^{-9}$ and extremely low ($12D$ is the energy of formation of a simple vacancy, and is related to the removal of a single atom from a close packed condensed system). The change in the density of the crystal heated below the melting point is also determined by the anharmonicity of the vibrations of the atoms. The increase in the temperature results in an increase in the distance between nearest neighbors. At zero temperature the density of the crystal is $\rho_0 = \sqrt{2}\,m/a^3$, where m is the atomic mass and a is the interatomic distance in the diatomic molecule in the ground state. The relative change in the density as the temperature is raised from zero the melting point of the crystal is $1 - (\rho_s/\rho_0)$ where ρ_s is the density of the crystal at the melt-

TABLE XVII. Reduced parameters of the condensed state of inert gases at the melting temperature.

	Ne	Ar	Kr	Xe	Average
$1-(\rho_l/\rho_s)$	0.137	0.126	0.136	0.131	0.132 ± 0.005
$\Delta H_{melt}/D$	0.825	0.923	0.907	0.910	0.89 ± 0.04
E_{bub}/n	8.3	8.6	8.0	8.3	8.3 ± 0.2
n, Number of vacancies in a bubble	45	37	59	45	46± 9
η, Fraction of atoms on the surface of a bubble	0.209	0.205	0.190	0.200	0.201 ± 0.008

ing point. Table XVII lists the values of this parameter for the various inert gases.

The solid-liquid phase transition results in the formation of vacancies—bubbles—within the condensed system of atoms. Each bubble consists of one or more simple vacancies, that is, it corresponds to the removal of one or several atoms. This idea, which is taken here as the basic premise, has been developed by specialists in the physics of phase transitions (see, e.g., Ref. 108). We shall determine the average size of the bubbles that are formed in phase transitions of various inert gases, using general information on this process and the energy parameters of the clusters that are removed from the condensed system of atoms.

For this purpose we determine first the energy ε_{melt} per bond at the melting temperature. At zero temperature this quantity is equal to D, the dissociation energy of a diatomic molecule in the ground state. Since the melting temperature and the boiling temperature are close together, we assume that the energy per bond is the same at the two temperatures. Previously, we have found (formula (27)) that for different versions of the disorder model of the surface of a condensed system of atoms the evaporation energy of a single atom is $\varepsilon_{ev} = 6D$. Therefore, $\varepsilon_{ev}/6$ is the energy of a single bond at the boiling temperature, and hence also at the melting temperature. Table XVII gives the corresponding parameters for the different inert gases.

We use the data in Table XVII to determine the average parameters of the bubbles that are formed in the melting of a crystal of an inert gas. We assume that the bubble contains n simple vacancies, i.e., it is formed by the removal of n atoms from the crystal. The energy of formation of the bubble is

$$E_{bub} = 6nD + E_{sur}, \tag{50}$$

where E_{sur} is the surface energy of the removed cluster containing n atoms. The energy used in the formation of a simple vacancy, that is, the energy associated with the removal of one atom, is

$$\varepsilon_{bub} = E_{bub}/n = 6D + (E_{sur}/n), \tag{51}$$

where D is the energy per bond at the melting temperature. Figure 21 shows the variation of ε_{bub} as a function of n, obtained from the data for clusters with a face-centered cubic lattice.

On the other hand, it is possible to determine this quantity from measurements of the parameters of the plane transition. Denoting the density of the condensed system of atoms in the crystalline and the liquid states at the melting temperature as ρ_s and ρ_l, respectively, we find that in the phase transition the concentration of vacancies formed is $(\rho_s - \rho_l)/\rho_s$ (where ρ_l is the density of the liquid at the melting temperature), so that the density of simple vacancies (the number of atoms removed per unit volume of the material) is

$$N_{vac} = (1 - \rho_l/\rho_s)\cdot\sqrt{2}/a^3, \tag{52}$$

where a is the nearest-neighbor distance at the melting temperature ($\sqrt{2}/a^3$ is the density of atoms in a close packed structure). In addition, the heat of fusion ΔH_{melt} per unit volume of the material is a measurable quantity. Using this quantity, we find that the energy of formation of a simple vacancy is

$$E_{bub}/n = \Delta H_{melt}/N_{vac}. \tag{53}$$

Substituting expressions (51) and (52) into (53), we

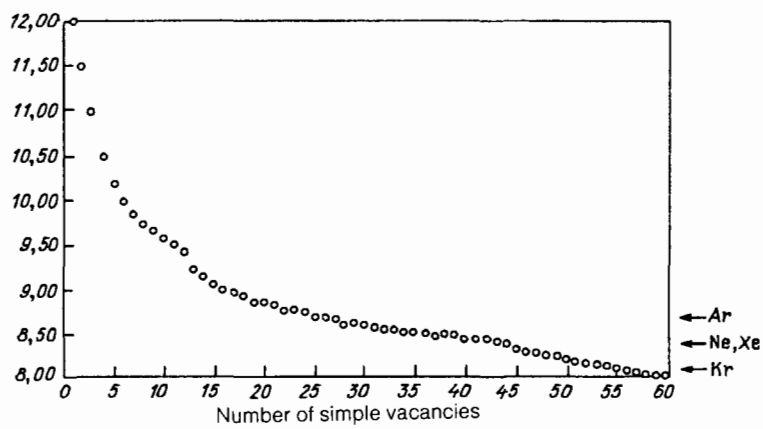

FIG. 21. Energy expended in the formation of a single simple vacancy (removal of one atom) as a function of the number of simple vacancies in a bubble (the number of atoms removed from the cluster) in a condensed system of atoms with close packing.

determine the average number of simple vacancies in the bubbles formed in the melting of inert gas crystals. The corresponding results are given in Table XVII and Fig. 21. The number of vacancies in a bubble is surprising. This fact will not be discussed here; we shall leave to more competent specialists to analyze this conclusion and find whether the large number of vacancies in a bubble is a general result.

The result takes into account the features of the model used, in which long-range interactions between atoms are neglected. Therefore, no stresses exist in a condensed system of atoms, including stresses incurred in the formation of the vacancies, and moreover, the vacancies do not interact among themselves. Above (in Sec. 3.1), it was shown that the observed energies of sublimation of condensed inert gases are closer to the energies given by this model than by the model of a condensed system with the Lennard–Jones interaction between atoms. A determination of the average number of vacancies in a bubble in a model system with the Lennard–Jones interaction gives an even higher number n for the number of simple vacancies in a bubble.

As can be seen, the liquid state corresponds to porous matter, and these pores inside the material allow the atoms to change their relative positions. From the parameters derived for the bubbles, we shall determine the parameters of this porous material. One of the basic characteristics of porous matter is the specific area of its internal surface. We shall introduce a similar characteristic that is convenient for understanding this physical phenomenon—the concentration η of atoms on the surface of a bubble, i.e., the fraction of the atoms situated on the surface of a bubble. A bubble is considered to be a macroscopic formation of radius r, so that if it contains n simple vacancies its radius can be found from the expression

$$n = \frac{4\pi r^3}{3} \cdot \frac{\sqrt{2}}{a^3} = \frac{4\pi\sqrt{2}}{3} \left(\frac{r}{a}\right)^3, \tag{54}$$

where $\sqrt{2}/a^3 = \rho_s/m$ is the density of atoms in the system; ρ_s is the density of the crystal at the melting temperature and m is the mass of an atom.

The relative number of atoms on the surface of a bubble is

$$\eta = \left(1 - \frac{\rho_l}{\rho_s}\right) \cdot \frac{4\pi r^2 a}{4\pi r^3/3} = \left(1 - \frac{\rho_l}{\rho_s}\right) \left(\frac{36\pi\sqrt{2}}{n}\right)^{1/3}, \tag{55}$$

where ρ_s and ρ_l are, respectively, the densities of the system in the solid and liquid state at the melting temperature of the crystal, and n is the average number of simple vacancies in a bubble. The numerical values of η for the different inert gases are listed in Table XVII. As can be seen, in liquid inert gases about 20% of the atoms are located on the surfaces of bubbles.

The parameters of a liquid, which is a porous object, change very rapidly with the temperature. For example, when the temperature of a liquid inert gas goes from the melting point to the boiling point at atmospheric pressure the fraction of the volume occupied by vacancies goes from $(13.2 \pm 0.5)\%$ to $(15.4 \pm 0.8)\%$. Since the melting temperature and the boiling temperature are close together, we assume that the change in the density of the liquid is due to the formation of new vacancies.

The presence of pores in a liquid alters its surface properties. Previously, we analyzed the surface tension, which is characterized by the force acting on the liquid-gas interphase surface.

Let us now analyze the change in the surface energy due to the crystal-liquid transformation. If we approximate the bubble by a sphere of definite radius and construct an arbitrary plane in the liquid, then the part of the area of this plane that lies within bubbles is $\Delta V/V$, where ΔV is the part of the selected volume V of liquid occupied by bubbles. This implies that the crystal-liquid phase transition reduces the specific surface energy of the condensed system of atoms with a short range interaction by about 13%. As can be seen, this change does not depend on the size of the bubbles that are formed, but is expressed in terms of the concentration of simple vacancies, that is, the number of atoms removed per unit volume of the structure.

Thus, at the melting temperature we obtain for the specific surface energy of a liquid at the melting point, in addition to formula (32), the formula

$$\varepsilon_{sur} = (1{,}69 \pm 0{,}12)\, D/a^2, \tag{56}$$

where D and a are the dissociation energy and the equilibrium internuclear distance of the diatomic molecule in the ground state.

6. CONCLUSIONS

The analysis carried out here shows the virtues and drawbacks of the model of a short range interaction between atoms. The short-range interaction, which, in the absence of a long-range interaction, has a steep variation in the potential in the repulsive part of the interaction and a shallow and narrow potential well in the attractive region, allows us to model the atoms by more or less hard balls. The model of the short-range interaction between the atoms is described well by a system of atoms with a repulsive exchange interaction. The most appropriate systems of this sort are the inert gases in the gaseous or the condensed states. Exotic systems of this type are metastable crystals[110] consisting of atoms of nonzero electron spin with the spins of all the atoms parallel, solid carbon consisting of C_{60} clusters,[68,69] etc. Systems of atoms with non-short-range (and consequently non-pairwise) interactions between the atoms can employ the results obtained for pairwise short range interactions as model systems.

However, the interest in atoms with a short range interaction is not due solely to the utility of the model. This model poses a number of fundamental questions that are easier to sort out within this simple model. It was shown above that scaling laws are obeyed better for condensed systems of inert gases than might be expected from general considerations. According to this scaling the various parameters of condensed systems of atoms can be expressed in terms of the parameter of the diatomic molecule, the dissociation energy, and the equilibrium internuclear distance in the molecule. However, the significant results that follow from an analysis of the experimental data make it much simpler to understand some fundamental regularities and obtain information on a number of topics.

The first of these is melting, which occurs at a temperature of $0.58D$ (Table VIII) and is a phase transition related to the loss of long-range order. The melting process is asso-

ciated with the formation of vacancies within the condensed system, and the transitions studied with the use of data on the parameters of the process provide information about these vacancies. Such information can be useful in a more thorough analysis of the process. Another topic of this type is the temperature dependence of the specific surface energy and the surface tension at temperatures near the melting point. Yet another problem is the transition to the critical point. All these issues can be analyzed in detail on the basis of the model studied here, which involves short-range (and consequently pairwise) interactions between the atoms.

It is clear that specialists have their own answers to questions of this sort, but the complexity of the methods that are involved do not always make the answers convincing to specialists in other fields of physics, while the fact that the number of systems to which these methods are applicable is limited makes the methods less than general. An understanding of these problems in the context of a simple model like a system of atoms with a short range interaction can make accessible to a broader range of scientists a simpler and more general means of description.

Let us point out the methodological aspect of the problem. The results presented in this review were obtained by analytical methods and from simple arguments. The incorporation of these ideas into present-day numerical methods[111,112] is a matter of fundamental importance. For example, the methods of molecular dynamics show that for a cluster the concept of a melting temperature is lost, because at some temperatures the atoms of the cluster can move freely near the surface of the cluster, whereas within the cluster the atoms are immobile.[113] If the liquid state is associated with the possibility that the atoms of the system can change their locations more or less frequently, then in a cluster the liquid and the solid state can coexist, and the melting temperature and the freezing temperature can be different.[114] The models presented here for the short-range interaction are well adapted to modern computer methods, and in particular they can be readily joined with the method of molecular dynamics. The use of modern computer methods in the context of the model described in this article opens up new possibilities for the understanding of the fundamental problems of the physics of clusters.

I would like to thank V. B. Leonas for valuable comments.

APPENDIX. SCATTERING CROSS SECTION IN A STEEPLY VARYING POTENTIAL

We define the differential and average scattering cross sections of atoms in the case of a steeply varying repulsive interaction potential between classical particles by using as a basis the potential of an infinite wall (Fig. 1). The scattering angle ϑ of classical particles is given by the relation[109]

$$\vartheta = \pi - 2\int_{r_0}^{\infty}\left(1-\frac{\rho^2}{R_2}-\frac{U(R)}{\varepsilon}\right)^{-1/2}\frac{\rho dR}{R^2}. \tag{A1}$$

Here ρ is the impact parameter of the collision, R is the distance between the particles, ε is the collision energy in the center of mass system, $U(R)$ is the interaction potential of the atoms, and r_0 is the distance of closest approach, which satisfies the relation

$$1-\frac{\rho^2}{r_0^2}-\frac{U(r_0)}{\varepsilon}=0. \tag{A2}$$

We expand the cross section in terms of the small parameter $1/n$, where $n = -\mathrm{d}\ln U(R)/\mathrm{d}R$. In the zero-order approximation we assume that $U(R)=0$, $R\geqslant r_0$, $U(R)=\infty$, $R\leqslant r_0$. From this we obtain

$$\vartheta = \pi - 2\arcsin\frac{\rho}{r_0} - 2\Delta\vartheta, \tag{A3}$$

$$\Delta\vartheta = \int_{r_0}^{\infty}\left[\left(1-\frac{\rho^2}{R^2}-\frac{U(R)}{\varepsilon}\right)^{-1/2} - \left(1-\frac{\rho^2}{R^2}\right)^{-1/2}\right]\frac{\rho dR}{R^2}. \tag{A4}$$

Relations (A3) and (A4) are exact. The expression used for the scattering angle is convenient, since in the present case $\Delta\vartheta\sim 1/n$. To avoid divergences in the calculation of the integral in Eq. (A4) we use the relation

$$-\frac{\mathrm{d}}{\mathrm{d}\rho}\int_{r_0}^{\infty}\left[\left(1-\frac{\rho^2}{R^2}-\frac{U(R)}{\varepsilon}\right)^{1/2} - \left(1-\frac{\rho^2}{R^2}\right)^{1/2}\right]\mathrm{d}R$$
$$= -\frac{\mathrm{d}r_0}{\mathrm{d}\rho}\left(1-\frac{\rho^2}{r_0^2}\right)^{1/2}$$
$$+\int_{r_0}^{\infty}\left[\left(1-\frac{\rho^2}{R^2}-\frac{U(R)}{\varepsilon}\right)^{-1/2} - \left(1-\frac{\rho^2}{R^2}\right)^{-1/2}\right]\frac{\rho dR}{R^2},$$

from which we obtain

$$\Delta\vartheta = \frac{\mathrm{d}r_0}{\mathrm{d}\rho}\left(1-\frac{\rho^2}{r_0^2}\right)^{1/2}$$
$$-\frac{\mathrm{d}}{\mathrm{d}\rho}\int_{r_0}^{\infty}\left[\left(1-\frac{\rho^2}{R^2}-\frac{U(R)}{\varepsilon}\right)^{1/2} - \left(1-\frac{\rho^2}{R^2}\right)^{1/2}\right]\mathrm{d}R. \tag{A5}$$

Taking into account that the last integral converges near $R\equiv r_0 (R-r_0\sim 1/n)$, we determine the integral with an accuracy to $1/n$:

$$\int_{r_0}^{\infty}\left[\left(1-\frac{\rho^2}{R^2}\right)^{1/2} - \left(1-\frac{\rho^2}{R^2}-\frac{U(R)}{\varepsilon}\right)^{1/2}\right]\mathrm{d}R$$
$$\approx \left(1-\frac{\rho^2}{r_0^2}\right)^{1/2}\int_{r_0}^{\infty}\left\{1-\left[1-\left(\frac{r_0}{R}\right)^n\right]^{1/2}\right\}\mathrm{d}R$$
$$= \left(\rho^2-r_0^2\right)^{1/2}\int_0^1\frac{1-(1-x)^{1/2}}{nx^{1+(1/n)}}\mathrm{d}x = \frac{2}{n}(1-\ln 2)\left(r_0^2-\rho^2\right)^{1/2},$$

where

$$x = \frac{U(R)}{\varepsilon}\left(1-\frac{\rho^2}{r_0^2}\right)^{-1} = \frac{r_0^n}{R^n}.$$

From this result we obtain

$$\Delta\vartheta = \frac{\mathrm{d}r_0}{\mathrm{d}\rho}\left(1-\frac{\rho^2}{r_0^2}\right)^{1/2} + \frac{2(1-\ln 2)}{n}\frac{\mathrm{d}}{\mathrm{d}\rho}\left(r_0^2-\rho^2\right)^{1/2}. \tag{A6}$$

Formulas (A2), (A3), and (A6) allow us to find an expression for the scattering angle in the case where the repulsive potential varies steeply. Introducing the variable $u = U(r_0)/\varepsilon$, we have on the basis of those formulas

$$\vartheta = 2\arcsin u^{1/2} - 2\left[\frac{2-(n-2)\ln 2}{n}\right]\frac{[u(1-u)]^{1/2}}{1+[(n-2)u/2]}$$
$$\approx 2\arcsin^{1/2} - 2\ln 2\,\frac{[u(1-u)]^{1/2}}{1+(nu/2)}, \qquad (A7)$$

where $n = -\mathrm{d}\ln u/\mathrm{d}\ln r_0$. This expression has an independent meaning, allowing us to find the dependence of the scattering angle on the collision impact parameter ρ, which is related to the distance of closest approach r_0 by formula (A2):

$$u = 1 - \left(\rho^2/r_0^2\right). \qquad (A8)$$

In the calculation of the differential scattering cross section it is assumed that the main contribution to the cross section comes from the range of values $u \sim 1$, where expression (A7) has the form

$$\vartheta = 2\arcsin u^{1/2} - \frac{4\ln 2}{n}\left(\frac{1-u}{u}\right)^{1/2}. \qquad (A9)$$

Under the assumption that the second term is small, we have with an accuracy to terms of order $1/n$

$$\sigma^{(1)} = \int_0^\infty (1-\cos\vartheta)\cdot 2\pi\rho\,\mathrm{d}\rho$$
$$= \pi\int 2u\left[(1-u)\,\mathrm{d}r_0^2 - r_0^2\mathrm{d}u\right]$$
$$+ \pi\int_0^1 \frac{4\ln 2}{n}\left(\frac{1-u}{u}\right)^{1/2}\cdot 2\left[u(1-u)\right]^{1/2} r_0^2\mathrm{d}u\,.$$

On the basis of formula (A8), we have used the relation $\mathrm{d}\rho^2 = (1-u)\mathrm{d}r_0^2 - r_0^2\mathrm{d}u$ and have assumed that the first term is by a factor of $\sim 1/n$ smaller than the second. Carrying out the integration over u in the first term by parts and noting that $\rho = 0$ corresponds to $u = 1$ and $\rho = \infty$ corresponds to $u = 0$, we have

$$-\int_1^0 2\pi r_0^2 u\mathrm{d}u = \pi R_0^2 u^2\Big|_0^1 - \int \pi u^2\cdot 2r_0\mathrm{d}r_0$$
$$= \pi R_0^2 + \int_0^1 2\pi u r_0^2\mathrm{d}u/n = \pi R_0^2(1+n^{-1}),$$

where $u(R_0) = 1$, i.e., $U(R_0) = \varepsilon$. Repeating these calculations for the other integrals and keeping only terms of order $\sim 1/n$, we obtain finally

$$\sigma^{(1)} = \pi R_0^2\left(1 + \frac{3-4\ln 2}{n}\right). \qquad (A10)$$

We write the differential cross section in the form $\sigma^{(1)} = \pi R_1^2$, i.e.,

$$R_1 = R_0 + \left[(1{,}5 - 2\ln 2)/n\right].$$

We have

$$u(R_1) = (R_0/R_1)^n \approx \exp(-3/2 + 2\ln 2)$$
$$= 4\exp(-3/2) = 0{,}89.$$

Consequently, the differential cross section is[16,18]

$$\sigma^{(1)} = \pi R_1^2$$

with

$$\frac{U(R_1)}{\varepsilon} = 0{,}89. \qquad (A11)$$

Let us now average the cross section over a Maxwellian distribution of the particles. We determine the average cross section that figures in the expression for the diffusion coefficient (see formula (9))

$$\sigma_1(T) = \frac{1}{2}\int_0^\infty \sigma^{(1)}(\varepsilon)\,e^{-x}x^2\mathrm{d}x, \qquad (A12)$$

where $x = \varepsilon/T$ and T is the gas temperature. From formula (A11) it follows that $\sigma^{(1)}(\varepsilon) \sim \varepsilon^{-2/n}$, so that

$$\sigma^{(1)}(\varepsilon) = \sigma^{(1)}(\varepsilon_0)\,(\varepsilon\,\varepsilon_0^{-1})^{2/n}$$
$$= \sigma^{(1)}(\varepsilon_0)\left[1 - \left(\frac{2}{n}\right)\ln(\varepsilon\varepsilon_0^{-1})\right]. \qquad (A13)$$

This formula is valid in the region $\varepsilon \sim \varepsilon_0$, where the second term is considerably smaller than the first. Substituting (A13) into (A12) we obtain for the average cross section

$$\sigma_1(T) = \sigma^{(1)}(\varepsilon_0)\left[1 + \frac{2}{n}\ln(\varepsilon_0 T^{-1}) - \frac{1}{n}\int_0^\infty x^2\ln x\,e^{-x}\mathrm{d}x\right].$$

We choose the value of ε_0 such that the second and third terms cancel one another. We obtain $\varepsilon_0 = T\exp\psi(3)$, where $\psi(3) = -C + (3/2)$ is the derivative of the gamma function and $C = 0.577$ is Euler's constant. Thus, we have

$$\sigma_1(T) = \sigma^{(1)}\left[T\exp\left(-C + \frac{3}{2}\right)\right]$$

and taking into account formula (A11), we obtain for the average differential cross section

$$\sigma_1 = \pi r_1^2$$

for

$$\frac{U(r_1)}{T} = 4e^{-C} = 2{,}25. \qquad (A14)$$

Going through similar operations, we obtain for the cross section that goes into the expression for the thermal conductivity and the viscosity in the case of a steeply varying interaction potential between the atoms:

$$\sigma^{(2)} = \int(1-\cos^2\vartheta)\,\mathrm{d}\sigma = 2\pi R_2^2/3$$

with

$$U(R_2)/\varepsilon = 0{,}23. \qquad (A15)$$

The average cross section that goes into the expression for the thermal conductivity (7) and the viscosity (8) is

$$\sigma_2 = 2\pi r_2^2/3$$

for

$$U(r_2)/T = 0.83.$$

[1)] A statistical analysis of the data of Table VIII gives a value $T_m/D = 0.58 \pm 0.01$ for the ratio of the melting temperature T_m of an inert gas crystal to the dissociation energy D of a dimer. This ratio was used in Ref. 44 to estimate the melting temperature of carbon made up of C_{60} clusters.

[2)] For argon they can be shifted by one unit, since an Ar_2^+ ion can be at the center of the cluster instead of an Ar^+.[97,98]

[1] J. O. Hirschfelder, C. F. Curtiss, and R. B. Bird, *Molecular Theory of Gases and Liquids*, Wiley, New York (1954) [Russ. transl., IL., M. 1961].
[2] S. Chapman and T. G. Cowling, *The Mathematical Theory of Non-Uniform Gases. An Account of the Kinetic Theory of Viscosity, Thermal Conduction, and Diffusion in Gases*, Cambridge University Press, Cambridge (1952) [Russ. transl., IL., M., 1960].
[3] J. H. Ferziger and H. G. Kasper, *Mathematical Theory of Transport Phenomena in Gases*, North-Holland, (1972) [Russ. transl. IL., M., 1976].
[4] R. J. Le Roy, M. L. Klein, and I. J. McGee, Mol. Phys. **28**, 87 (1974).
[5] R. A. Aziz and H. H. Chen, J. Chem. Phys. **67**, 5719 (1977).
[6] G. C. Maitland, M. Rigby, E. B. Smith, and W. A. Wakeham, *Intermolecular Forces*, Clarendon Press, Oxford (1981).
[7] R. A. Aziz, in *Inert Gases: Potentials, Dynamics, and Energy Transfer in Doped Crystals*, M. Klein (ed.) Springer-Verlag, Berlin (1984).
[8] A. A. Radzig and B. M. Smirnov, *Reference Data on Atoms, Molecules, and Ions*, Springer-Verlag, Berlin, Heidelberg, New York (1985).
[9] K. P. Hubek and G. Herzberg, *Molecular Spectra and Molecular Structure IV: Constants of Diatomic Molecules*, Van Nostrand, Princeton, 1979.
[10] N. Schweitner, E. E. Koch, and J. Jortner, *Electronic Excitations in Condensed Gases*, Springer-Verlag, Berlin, Heidelberg, N. Y., 1985.
[11] A. A. Radgiz and B. M. Smirnov, *Parameters of Atoms and Atomic Ions* [in Russian], Energoatomizdat, M., 1986.
[12] S. H. Patil, J. Phys. B **20**, 3075 (1987).
[13] A. D. McLean, B. Liu, and J. A. Barker, J. Chem. Phys. **89**, 6339 (1988).
[14] V. B. Leonas, Usp. Fiz. Nauk **107**, 29 (1972) [Sov. Phys. Usp. **15**, 266 (1972)].
[15] B. M. Smirnov, *Asymptotic Theory of Atomic Collisions* [in Russian], Atomizdat, M., 1973.
[16] E. E. Nikitin and B. M. Smirnov, *Atomic-Molecular Processes* [in Russian], Nauka, M., 1988.
[17] E. E. Nikitin and B. M. Smirnov, *Slow Atomic Collisions* [in Russian], Energoatomizdat, M., 1990.
[18] B. M. Smirnov, Usp. Fiz. Nauk **138**, 517 (1982) [Sov. Phys. Usp. **25**, 854 (1982)].
[19] L. A. Palkina, B. M. Smirnov, and M. I. Chibisov, Zh. Eksp. Teor. Fiz. **56**, 340 (1969) [Sov. Phys. JETP **29**, 187 (1969)].
[20] L. A. Palkina and B. M. Smirnov, Teplofiz. Vys. Temp. **12**, 37 (1974) [High Temp. (USSR) **12**, 32 (1974)].
[21] A. V. Eletskiĭ, L. A. Palkina, and B. M. Smirnov, *Transport Phenomena In a Weakly Ionized Plasma* [in Russian], Atomizdat, M., 1975.
[22] E. W. McDaniel and E. A. Mason, *The Mobility and Diffusion of Ions in Gases*, Wiley, New York, (1973) [Russ. transl. IL., M., 1976].
[23] T. Kihara, M. H. Taylor, and H. O. Hirschfelder Phys. Fluids **3**, 715 (1960).
[24] L. D. Higgins and F. J. Smith, Mol. Phys. **14**, 399 (1968).
[25] F. J. Smith, E. A. Mason and R. J. Munn, J. Chem. Phys. **42**, 1334 (1965).
[26] A. B. Kamnev and V. B. Leonas, Dokl. Akad. Nauk SSSR **165**, 1273 (1965) [Sov. Phys. Dokl. **10**, 1202 (1965)].
[27] Yu. N. Belyaev and V. B. Leonas, Dokl. Akad. Nauk SSSR **173**, 306 (1967) [Sov. Phys. Dokl. **12**, 233 (1967)].
[28] L. J. Danielson and M. Keil, J. Chem. Phys. **88**, 851 (1988).
[29] N. B. Vargaftik, L. P. Filippov, A. A. Tarzimanov, and E. E. Totskiĭ, *Handbook of Thermal Conductivity of Liquids and Gases* [in Russian], Energoatomizdat, M., 1990.
[30] N. B. Vargaftik, *Handbook of Thermophysical Properties of Gases and Liquids* [in Russian], Nauka, M. (1972).
[31] W. Hogervorst, Physica **51**, 59 (1971).
[32] C. J. Zwakhals and K. W. Reus, Physica C **100**, 231 (1980).
[33] W. L. Taylor and D. Cain, J. Chem. Phys. **78**, 6220 (1983).
[34] B. Stefanov, L. Zarkova, and D. Oliver, Teplofiz. Vys. Temp. **14**, 56 (1976) [High Temp. (USSR) **14**, 48 (1976)].
[35] L. D. Landau and E. M. Lifshitz, Statistical Physics, 2 Vols. 3rd ed. Pergamon Press, Oxford, 1980 [Russ. original, Nauka, M., 1976].
[36] H. E. Stanley, *Introduction to Phase Transitions and Critical Phenomena*, Oxford University Press, N.Y., 1971 [Russ. transl., Mir, M., 1973].
[37] V. G. Baĭdakov, *Reviews of the Thermophysical Properties of Matter*, No. 69 [in Russian], High-Temperature Institute, Academy of Sciences of the USSR, M., 1988.
[38] A. J. Moses, *The Practicing Scientist's Handbook*, Van Nostrand and Reinholt, N. Y, 1978.
[39] R. E. Honig and H. O. Hook, RCA Rev. **21**, 360 (1960).
[40] C. Kittel, *Introduction to Solid State Physics, 6th ed.*, John Wiley, N. Y. 1986 [Russ. transl., Fizmatgiz, M., 1963].
[41] G. Leibfried, "Gittertheorie der mechanischen und thermischen Eigenschaften der Kristalle" in *Handbuch de Physik*, S. Flugge (ed.), Vol. 7, Part 1, Springer-Verlag, Berlin, 1955 [Russ. transl., Fizmatgiz, M., 1963].
[42] C. W. Bunn, *Crystals*, Academic Press, N.Y., 1964 [Russ. transl., Fizmatgiz, M., 1963].
[43] N. W. Ashcroft and N. D. Mermin, *Solid State Physics*, Saunders College, Philadelphia, 1976 [Russ. transl., Mir, M., 1970].
[44] A. V. Eletskiĭ and B. M. Smirnov, Usp. Fiz. Nauk **161**, 173 (1991) [Sov. Phys. Usp. **34**, 616 (1991)].
[45] T. Ichihashi, K. Tanijaki, T. W. Ebbsnsen *et al.*, Chem. Phys. Lett. **190**, 179 (1992).
[46] C. Ono and C. Kondo, "Molecular Theory of Surface Tension in Liquids" in *Encyclopedia of Physics*, S. Flugge (ed.), Vol. 10 (1960).
[47] J. S. Rowlinson and B. Widom, *Molecular Theory of Capillarity*, Clarendon Press, Oxford, 1982 [Russ. transl., Mir, M., 1986].
[48] A. I. Rusanov, *Phase Equilibria and Surface Phenomena* [in Russian], Khimiya, L., 1967.
[49] V. K. Seminchenko, *Surface Phenomena in Metals and Alloys* [in Russian], Gostekhizdat, M., 1957.
[50] Landolt-Bornstein, Phys. Chem. Tabellen. Bd. 1. Springer-Verlag, Berlin, Heidelberg, New York, 1973, p. 198.
[51] *Encyclopedia of Sciences and Technology*, Vol. 13, McGraw-Hll, N. Y. 1960.
[52] R. C. Weast (ed.), *Handbook of Chemistry and Physics, 70th ed.*, CRC Press, Inc., Boca Raton, 1989, 1990, p. 20.
[53] S. Sugano, Y. Nishina, and S. Ohnishi (eds.), *Microclusters*, Springer-Verlag, Berlin, 1987.
[54] P. Jena, B. K. Rao, and S. N. Khana, *Physics and Chemistry of Small Clusters*, Plenum Press, N. Y., 1987.
[55] G. Benedek and M. Pachioni (eds.), *Elemental and Molecular Clusters*, Springer-Verlag, Berlin, 1988.
[56] E. R. Bernstein (ed.), *Atomic and Molecular Clusters*, Elsevier, Amsterdam, 1990.
[57] V. M. Smirnov, *Cluster Ions and van der Waals Molecules*, Gordon and Breach, Philadelphia, 1992.
[58] W. D. Knight *et al.*, Phys. Rev. Lett. **52**, 2141 (1984).
[59] W. Ekardt, Ber. Bunsenges. Phys. Chem. **88**, 289 (1984).
[60] A. Herrmann, S. Leutwyler, E. Schumacher, and L. Woste, Helv. Chim. Acta **61**, 453 (1978).
[61] A. Herrmann, E. Schumacher, and L. Woste, J. Chem. Phys. **68**, 2327 (1978).
[62] H. Golich, T. Lange, T. Bergman, and T. P. Martin, Phys. Rev. Lett. **65**, 748 (1990).
[63] S. Bjornholm, J. Borggreen, O. Echt, K. Hansen, J. Pedersen and H. D. Rasmussen, Phys. Rev. Lett. **65**, 1627 (1990).
[64] T. P. Martin, T. Bergman, H. Gohlich, and T. Lange, Chem. Phys. Lett. **172**, 209 (1990).
[65] S. Bjornholm, J. Borggreen, O. Echt, K. Hansen, J. Pedersen, and H. D. Rasmussen, Z. Phys. **19**, 47 (1991).
[66] T. P. Martin, T. Bergman, H. Gohlich, and T. Lange, Z. Phys. **19**, 25 (1991).
[67] H. Gohlich, T. Lange, T. Bergman, U. Naher, and T. P. Martin, Chem. Phys. Lett. **187**, 67 (1992).
[68] F. Curl and R. E. Smalley, Sci. Am. **265**(4), 54 (October 1991).
[69] D. R. Huffman, Phys. Today **44**(11), 22 (November 1991).
[70] D. A. Jelski, Z. C. Wu, and T. F. George, J. Cluster Sci. **1**, 147 (1990).
[71] C. L. Cleveland and U. Landman, J. Chem. Phys. **94**, 7376 (1991).
[72] B. K. Teo and H. Zhang, J. Cluster Sci. **1**, 155 (1990).
[73] B. M. Smirnov, Usp. Fiz. Nauk **162**, 119 (1992) [Sov. Phys. Usp. **35**, 37 (1992)].
[74] M. R. Hoare, Adv. Chem. Phys. **40**, 49 (1979).
[75] M. R. Hoare and J. A. McInnes, Adv. Phys. **32**, 791 (1983).
[76] S. W. Wang, L. M. Falikov, and A. W. Searcy, Surf. Sci. **143**, 609 (1984).
[77] J. A. Northby, J. Chem. Phys. **87**, 6166 (1987).
[78] J. W. Lee and G. D. Stein, J. Phys. Chem. **91**, 2450 (1987).
[79] H. G. Fritsche, Phys. Stat. Solidi B **143**, K11 (1987).
[80] J. D. Honeycutt and H. C. Andersen, J. Phys. Chem. **91**, 4950 (1987).
[81] B. Raoult, J. Farges, M. F. de Feraudy, and G. Torchet, Philos. Mag. B **60**, 881 (1989).
[82] B. W. van de Waal, J. Chem. Phys. **90**, 3407 (1989).
[83] J. Farges, M. F. de Feraudy, B. Raoult, and G. Torchet, Surf. Sci. **106**, 95 (1981).
[84] J. Farges, M. F. de Feraudy, B. Raoult, and G. Torchet, J. Chem. Phys. **78**, 55067 (1983).

[85] J. Farges, M. F. de Feraudy, B. Raoult, and G. Torchet, Adv. Chem. Phys. **70**, part 2, 45 (1988).
[86] A. L. Mackay, Acta Crystallogr. **15**, 916 (1962).
[87] O. Echt, K. Sattler, and E. Recknagel, Phys. Rev. Lett. **47**, 1121 (1981).
[88] O. Echt *et al.*, Ber. Bunsenges. Phys. Chem. **86**, 860 (1982).
[89] A. Ding and J. Hesslish, Chem. Phys. Lett. **94**, 54 (1983).
[90] J. Farges, M. F. de Feraudy, B. Raoult, and G. Torchet, J. Chem. Phys. **78**, 5067 (1983).
[91] E. Recknagel *et al.*, Ber. Bunsenges. Phys. Chem. **88**, 201 (1984).
[92] J. Farges, M. F. de Feraudy, B. Raoult, and G. Torchet, J. Chem. Phys. **84**, 3491 (1986).
[93] T. D. Mark and P. Scheier, Chem. Phys. Lett. **137**, 245 (1987).
[94] W. Miehle, O. Kandler, T. Leisner, and O. Echt, J. Chem. Phys. **91**, 5940 (1989).
[95] P. G. Lethbridge and A. J. Stace, J. Chem. Phys. **91**, 7685 (1989).
[96] T. P. Martin, T. Bergman, H. Gohlich, and T. Lange, Chem. Phys. Lett. **177**, 343 (1991).
[97] J. M. Soler, J. J. Saenz, N. Garcia, and O. Echt, Chem. Phys. Lett. **109**, 71 (1984).
[98] H. Haberland, Surf. Sci. **156**, 305 (1985).
[99] B. M. Smirnov, Usp. Fiz. Nauk **161**(6), 171 (1991) [Sov. Phys. Usp. **34**, 526 (1991)].
[100] J. Fricke (ed.), *Aerogels*, Springer-Verlag, Berlin, New York, Heidelberg, 1986.
[101] B. M. Smirnov, Phys. Rep. **188**, 1 (1990).
[102] A. A. Lushnikov, A. E. Negin, and A. V. Pakhomov, Chem. Phys. Lett. **175**, 138 (1990).
[103] A. A. Lushnikov, A. E. Negin, A. V. Pakhomov, and B. M. Smirnov, Usp. Fiz. Nauk **161**(2), 113 (1991) [Sov. Phys. Usp. **34**, 160 (1991)].
[104] S. Henning, in *Aerogels*, J. Fricke (ed.), Springer-Verlag, Berlin, Heidelberg, New York, 1986.
[105] M. Kh. Karapet'yants and M. L. Karapet'yants, *Principal Thermodynamic Constants of Inorganic and Organic Materials* [in Russian], Khimiya, M., 1968.
[106] C. A. M. Mulder and J. G. van Lierop, in *Aeorgels*, J. Fricke (ed.), Springer-Verlag, Berlin, Heidelberg, New York, 1986.
[107] A. R. Ubbelohde, *Melting and Crystal Structure*, Clarendon Press, Oxford, 1962 [Russ. transl. Mir, M., 1969].
[108] A. G. Khrapak, Pis'ma Zh. Eksp. Teor. Fiz. **47**, 372 (1988) [JETP Lett. **47**, 445 (1988)]; Pis'ma Zh. Eksp. Teor. Fiz. **51**, 403 (1990) [JETP Lett. **51**, 457 (1990)].
[109] L. D. Landau and E. M. Lifshitz, *Mechanics, 3rd ed.*, Pergamon Press, Oxford, 1976 [Russ. original, Nauka, M., 1973].
[110] B. M. Smirnov and G. V. Shlyapnikov, Usp. Fiz. Nauk **120**, 691 (1976) [Sov. Phys. Usp. **19**, 1023 (1976)].
[111] R. Jullien, L. Peliti, R. Rammal, and N. Boccara (eds.), *Universalities in Condensed Matter*, Springer-Verlag, Berlin, New York, Heidelberg, 1988.
[112] D. P. Landau, K. K. Mon, and H. B. Schuttler (eds.), *Computer Simulation Studies in Condensed Matter Physics*, Springer-Verlag, Berlin, New York, Heidelberg, 1988.
[113] U. Landman, in *Computer Simulation Studies in Condensed Matter Physics*, D. P. Landau, K. K. Mon, and H. B. Schuttler (eds.), Springer-Verlag, Berlin, New York, Heidelberg, 1988, p. 108.
[114] R. S. Berry, Sci. Am. **263**(2), 68 (August 1990).

Translated by J. R. Anderson